THE DEVELOPMENT OF A PORTABLE VESSEL FOR THE COLLECTION, STORAGE, AND UTILIZATION OF SOLAR THERMAL ENERGY FOR HOUSEHOLD USE

BY

MATTHEW PAUL ALONSO

DISSERTATION

Submitted in partial fulfillment of the requirements
for the degree of Doctor of Philosophy in Agricultural and Biological Engineering
in the Graduate College of the
University of Illinois at Urbana-Champaign, 2018

Urbana, Illinois

Doctoral Committee:

Professor J. Bruce Elliott-Litchfield, Chair
Professor Tami Bond
Professor Madhu Viswanathan
Professor Prasanta Kalita

Abstract

The purpose of this work is to address the global need for a cooking system without fuel, fire, or emissions and that respects cultural norms and cooking traditions. 3 billion people cook on wood, animal dung, and charcoal. The emissions from burning these fuels cause over 4 million premature deaths a year and negatively impact our environment. In addition, the energy impoverished spend ~25% of their income on household fuels. Solar energy can provide a solution and do so in a culturally appropriate manner.

Stored solar thermal energy can provide an option to: cook at any time or place; replace the fuel and the fire in most cooking systems; and perform similar to fire cooking. This dissertation documents the first sealed portable solar thermal energy storage vessel that operates in the 300 - 400 °C range. This is quantified by measuring the performance of a field tested solar thermal energy system and through laboratory testing of the thermal energy storage vessel.

Field tests measured the temperature - time relationship during solar heating of storage vessels to 340 °C and the recovery of energy from these vessels using a water heating test. Each vessel contained 5 kg of potassium nitrate and were composed of 1.7 kg of aluminum. They were heated with low cost, commercially available and unmodified, 1.5 m^2 parabolic solar cookers. The energy storage vessels were heated in an average time of 2 hours and 21 minutes. During energy recovery testing, the solar charged vessels heated an average of 7 L of water, totaling about 2.3 MJ of useful cooking energy. The first liter of water reached “boiling” temperature (95 °C) in an average of 3 minutes and 40 seconds.

The portable thermal energy storage vessel was used as a platform to test additional energy storage materials. The thermal energy recovery performance capabilities of aluminum, potassium nitrate, sodium nitrate, and a 60/40 mol% mixture of sodium nitrate and potassium nitrate were experimentally measured. Between 2.2 - 2.9 MJ of energy were recovered from these vessels. They boiled 6 - 9 L of water. The initial power output of the vessels ranged from 1000 - 2000 W. In addition, a discussion on evaluating the performance of stored solar thermal energy systems was initiated. Future work can compare the documented performance of these materials with the local cooking requirements to select an appropriate thermal storage solution for the community.

The results are promising for the development of stored solar thermal energy systems for cooking and other small-scale uses of thermal energy including space heating, food processing, device charging and lighting.

To my family, mi familia, and to the F.I.R.S.T. Robotics program (Go Team 81).

Everything I am stems from you.

Acknowledgments

I am deeply grateful for the support, mentorship, and friendship I've found in the Urbana-Champaign community. Thank you to the Morrill Engineering Program - the late Dean Paul Parker, Jonne Brown, Brenda Leon, and the supporters of MEP - your advise, smiling faces, and support were invaluable to me and my success here. To the former Office of Special Programs in the College of Engineering and its champion Dr. Susan Linnemeyer, engineering outreach is my rock and your inclusion of me in that effort kept me whole. Thank you for reaching out to those whose lives were touched by me and showing me what impact I could have in the world. I thank Dr. Ty Newell and Dr. Emad Jassim as many of my professional opportunities stemmed from their inclusion of me in their research efforts. I will always appreciate their guidance, mentorship, and investment in community.

During my transition away from and back to academia, Joe Muskin, Dean Ivan Favila, and Dr. Charles Tucker provided valuable guidance and support. Joe, I am so happy to have met you and have spent countless hours learning from you. You are an amazing educator, your boundless energy has always been in inspiration to me, and I have learned much about life from your stories. Professor Tucker, thank you for sharing your professional challenges with me as that openness has made me a better mentor and teacher. I've since learned how valuable it is for students to hear of "failures" from those who have succeeded. Thank you both again for helping me learn more about the importance of being humble and sharing life's ups and downs. Thank you to Ivan for mentoring me during our racquetball sessions and for trusting me to work with students.

My return to complete my Ph.D. wouldn't have been possible without the innovative programs created by Dr. J. Bruce Elliott-Litchfield and my friendship with Steve Granda. Option C rebuilt my confidence, allowed me to explore my passions, and learn about who I am. My success in the laboratory was made possible by the students I worked with. Catherine Zhou, having you in the lab enhanced my focus, my organization, and my spirits. I wish you immeasurable success in life and

I hope graduate school is an enjoyable experience for you. Thank you to Blake and Rachel for your dedication to your laboratory work and your assistance in exploring thermal storage. An additional thank you to the numerous undergraduate students who spent time with me in the laboratory; I appreciated your ideas, your insights, and your curiosity.

Thank you to Dr. Madhu Viswanathan for training me how to work in subsistence marketplaces. Like others I've highlighted here, your character is incredibly inspiring and interacting with you was immensely valuable to my growth and well-being. It was an honor to have you on my committee and to be your student.

To Dr. Tami Bond, thank you for serving on my committee and for being a role-model to me. I am very appreciative of your comments on my dissertation and your guidance. Your critical thinking skills and commitment to sustainability are admirable and encourage me to strive to a higher standard.

To Dr. Prasanta Kalita, thank you joining my committee and for supporting my work. I admire the passion that you bring to your work and the good nature of your character. Thank you again for everything that you do to solve inequitable situations around the world and for graduate students here at Illinois.

Thank you to the entire Sun Buckets team for your support and your contributions to Sun Buckets. Having an entrepreneurial outlet for this work kept me focused on the significant impact we can have on the world.

Para mi abuela, Maria, mi tío abuelo Ricardo y mi tía abuela Ana: Thank you for instilling a love for education in your children, your grandchildren, your nieces and nephews, your great nieces and nephews, in short - your whole family. Your message was heard loud and clear, and we have all benefited immensely from it. It is a message I will share widely and freely.

To my siblings, I would not have made it without you. Karlena, you led us to success in our lives and higher education - I thank you dearly. Mike, you've been here and your help in navigating graduating school and improving my writing is deeply appreciated. Even in this, my acknowledgements, I looked to you for inspiration. Jeremy, through everything I've always had you to support me and to help me reason my through life. I thank you dearly. To my friends who are my brothers, Jason and Ferny, I'm honored to be a part of your lives - uncle and tío to your amazing children. Ferny, you hold me accountable to my life and keep me in check, thank you. Jason, thank you for always having my back and for our crazy discussions growing up. I have no doubt they helped nurture a love for engineering before either of us knew what that was. To my Crister, thank you for holding me accountable and reminding me I need to get it done while simultaneously encouraging me to relax.

To Mom and Dad, thank you for your love and support. You gave me the freedom to explore life and to make mistakes with the knowledge and comfort that my parents would always be there for me. From Hooked On Phonics to my Ph.D., I've had your support. To Keith, thank you for teaching me patience and how to work with my hands. I've used these interpersonal skills to work with others and the technical skills to conduct my experiments. Para Marco y Paty, gracias por su amor y apoyo.

To my spouse, Dr. Renata Revelo, thank you for your love, your support, your wisdom, and for your patience. Thank you for insisting we travel and clear our heads for a few weeks every year as these memories will last us a lifetime.

My deepest appreciation and thanks goes to Bruce for his guidance in life and on this project. I also thank him for his extensive suggestions that improved my dissertation. I am honored to have been your student. Through working with you, I have become a better person, a better instructor, and a better thinker.

I interviewed people from around the world for this work. I am indebted to them for sharing intimate details about their lives with me and my colleagues. I hope this work is successful in alleviating the burdens associated with the global cooking problem.

Table of Contents

1 Introduction

This research is motivated by the challenges surrounding cooking - health issues, high fuel cost, gender-based violence during fuel collection - and other issues faced by energy-impoverished individuals around the world. My first exposure to this problem occurred in 2010 when I encountered my grandmother-in-law cooking on an indoor wood fire in La Paz, in the Carchi province of Ecuador. This first-hand exposure and understanding of this global problem was an awakening moment, and this work serves to improve the condition of individuals like her.

1.1 The Global Cooking Problem

According to the World Health Organization, 3 billion people use solid fuels like wood, animal dung, and charcoal as their primary fuel source. The emissions from burning these fuels cause over 4 million premature deaths a year from stroke, ischaemic heart disease, chronic obstructive pulmonary disease, and lung cancer [1]. The proportions and locations of these deaths are summarized in figure 1.1. 460,000 of these deaths are children under 5 who succumb to pneumonia [2]. In 2010, household air pollution from solid fuel cookfires was attributed to the loss of 119 million disability-adjusted life years (DALYS) [3]. The burning of solid fuels is a public health emergency in energy-impoverished areas. This problem is not just isolated to those cooking in their homes; the health impacts increase in urban areas where many people are using solid fuels. The particulates become concentrated in the air and impact entire communities of people, even those cooking with lower impact fuels like natural gas [3, 4].

In addition to the direct health impacts, cooking fires produce key global warming agents including carbon dioxide, black carbon, and ozone precursors. Reducing these emissions can have an immediate effect on climate change. Residential solid fuel cooking is responsible for one-third to one-half of global black carbon or about 10% of global climate forcing, while the CO_2 from these fires account for a further 10 - 20% [5, 6]. Though individual fires are small, the cumulative effects are sizable, and the personal, environmental, and public health impacts are tragic.

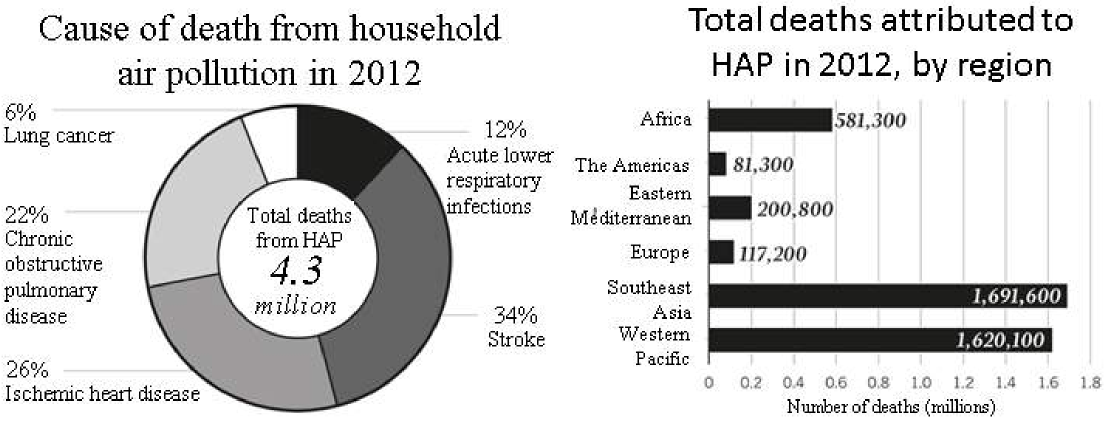

Figure 1.1: The cause of death and regions of impact, associated with household air pollution. Infographic adopted from Global Health: Deadly Dinners [7]

1.1.1 Solar as a Solution

The energy-impoverished live in communities with limited or unreliable clean energy solutions. Even when people can afford to pay for cleaner fuels, the infrastructure is often not available or suffers service disruptions. I interviewed women, in the Indian state of Tamil Nadu, who typically had to wait two weeks for a replacement gas cylinder. For some, wood is attractive because it can be freely collected or purchased at a very low cost and when it is available, it is a reliable source of fuel. However, the energy impoverished live in areas where solid fuels are becoming scarce and they increasing must purchase fuel. The Global Alliance for Clean Cookstoves and the World Bank estimate over 1 billion people currently pay for wood, charcoal, and/or coal. Overall, they estimate solid cooking fuels to cost between $100 - 250 USD/year per household, though some charcoal users are spending up to $400 USD/year in countries such as Haiti. They estimate a global average of 7% of income is spent on cooking and lighting fuel, while this increases to 10 - 20% for lower income households [8]. Similarly, the Asian Development Bank estimates that the poor spend between 25 - 30% of their household income on meeting their daily energy needs [9]. In addition, lost economic productivity and health expenses can increase these costs. There is a need for high value, healthy, and renewable off-grid cooking solutions.

The sun can provide a sustainable solution to this problem. It is abundant, providing more energy in under two hours than the global population consumes in a year. This energy is available in many of the same areas where the energy-impoverished reside, and it can provide an economical solution. Collecting solar energy has a fixed cost, the collector, and eliminates the variable cost of fuel that can be detrimental to low-income families. Solar energy lends itself to being collected by the user and can be used with limited resources, maintaining the user's agency.

In 1767, Horace de Saussure harvested the sun's energy, and was the first person to document the use of the sun to cook food [10]. In the years since, various solar cooker designs have been created that can bake, boil, and fry foods. Traditionally, they have been classified as box, panel, and concentrating solar cookers. Box- and panel-type cookers typically reach temperatures just above the boiling point of water, and work best when they are set up and left alone for several hours, cooking foods that require boiling or baking. They store low amounts of energy in the thermal mass of the structure and the air trapped inside. They can keep food warm for 1 - 2 hours after the sun has set, but cannot cook additional food during the evening.

Traditional methods of solar cooking have significant barriers and limitations. The drawbacks include cooking outside in the direct sunlight with a concentrating solar cooker or leaving food unattended for several hours to cook in an unfamiliar way. The user needs to adjust to cooking with a box or panel cooker, as it is very different from the high-heat and rapid cooking that is achieved when using fire. Parabolic and other concentrating cookers can be used for high-temperature cooking activities such as frying foods, but they only provide energy to cook when direct sunlight is available. The user has to remain outside, tending the food and adjusting the concentrator to track the sun. Regardless of the style of solar cooker used, the user cannot cook when, or where, they want. The behavior change necessary to adopt these technologies have been unacceptable for many individuals. This has led to solar cooking technologies having an abandonment rate of up to 90% globally [8].

This study researches key aspects for the development of a portable vessel to store solar thermal energy, namely the container design and means for sealing it, and the selection of the material(s) to be used inside the container to store the heat. The aim is to provide a clean source of energy on sunny days, energy that can be stored for use that evening or potentially several days after.

1.1.2 Adoption Factors

As part of the National Science Foundation Innovation Corps (NSF I-Corps) program and through a two-semester course in subsistence marketplaces, over 100 in-person interviews were conducted in India and the US, along with phone and video interviews conducted in India, Uganda, and the US. In the US, interviewees were identified through their connection to the solar cooking community or those who were camping at state parks. In India, we sought out women who identified as housewives and interviewed women in both rural and urban contexts. The Uganda participants were refugees in the Nakivale Refugee Camp who were identified by the Fuse Foundation. During the interviews information was collected on the consumer's lifestyle and economic class, cooking preferences and the associated costs, and how the user adopts new technology. Interviewees were also questioned about their attitude towards solar cooking and when appropriate, they were asked how they would view a high temperature, portable, solar charged cooking stove.

Interviewees wanted to be able to cook inside their home and cook rapidly. These interviews validated previous conclusions from failed solar energy interventions and information shared by non-governmental organizations (NGOs) [11]. This was the motivating principles for developing a portable, high temperature solar thermal storage system.

In certain regions, many people work when the sun is high in the sky. Other individuals are not accustomed to cooking during midday. In the state of Tamil Nadu in India for example, cooking often occurs in the late evening after the sun has set and in the very early morning before the sun rises. The noon meal is cooked in the morning and eaten cold. In addition, potential users aspired to improve their cooking situation and desired a cooking utensil that provides a feeling of improved social status. Many of the women interviewed who cooked on traditional wood stoves, similar to those in figure 1.2, hoped to acquire gas or induction stoves because of their ability to start instantly and cook rapidly. The petroleum fuel and electrical induction stoves, figure 1.3, satisfied this requirement but were costly to operate. Users reported monthly spending of ~1000 INR to cook on electric stoves, ~800 INR for gas, or ~200 INR to purchase firewood in Tamil Nadu. One user indicated the electric resistance stove, top center in figure 1.3, performed below her expectations and was discarded in favor of a traditional dung stove, pictured in figure 1.4.

In the past, a focus on producing low-cost stoves led to a wide variety of solar cooker designs

Figure 1.2: Wood and biomass stoves constructed out of mud and brick that were observed in the Indian state of Tamil Nadu.

Figure 1.3: Kerosene, gas, and electric stoves observed in the Indian states of Tamil Nadu and Haryana. Beginning at the top left and working clockwise the pictures are an example of a kerosene stove, electric resistance stove, an induction cooktop, another kerosene stove, and a gas range.

Figure 1.4: Animal dung cookstoves observed in the state of Haryana, India.

that have seen limited use and adoption. Solar Cookers International, a non-profit organization that promotes solar cooking globally, has been documenting solar cooker designs through a wiki that currently lists almost 400 products and designs [12]. Among these devices, there exists a design to accomplish almost any cooking task independently. To maintain their traditional cooking style, a particular user may need to use more than one solar cooker. For instance, they may need a box cooker to bake and a parabolic cooker to fry food. In addition, many solar cookers are do-it-yourself designs and tend to be perceived as being designed for "the poor". This perception reduces their adoption [13]. Commercially available solar devices overcome this perception, but are considered expensive because they have a high initial cost.

In 2013, Otte proposed a set of variables that influence the adoption of solar cookers. These variables focus on environmental factors (space availability, solar insolation, and the cost and availability of cooking fuels), cultural factors (preferred food characteristics, cooking habits, and daily cooking schedule), technical factors (performance, ease of use, and repairability), social factors (motivation for adoption - economic, health, and or environmental, perception of the technology, and power relationships in the community), economic factors and the political policies that affect them [13]. A device can fail by not meeting one set of these factors. Previous technology developers have focused on the technical ability to cook food, to process it with heat to the minimal extent that it is edible, without an emphasis on the cultural factors of potential users.

Central to many of the issues with solar cooking is the inability to store the solar energy. Contemporary cooking fuels - natural gas, wood, animal dung and other solid fuels - are essentially stored energy, and that property allows them to be used whenever and wherever needed. There is an acute need to develop a means to store solar thermal energy, which would address the environmental, cultural, and technical factors described by Otte. The solar community has recognized that energy storage is critical to match the needs of potential users and increase the adoption of solar cooking technology. The NGO Climate Healers released a challenge in March of 2011 for the engineering community to develop a solar cooker that works at night [14]. They identified this as the missing component to make solar cookers work in rural India. Cuce and Cuce in 2013, reviewed several solar cooking technologies and identified the inability to cook at night as the most challenging issue to address to spur adoption [15].

The solution developed in this work utilizes energy stored at high temperature, 300 - 400 °C. Operating at this temperature will provide the ability to sear, deep fry, pan fry, bake, and boil food using the tools and methods users are familiar with. Providing energy when needed in the daily cooking schedule and in a portable format that can be used inside or outside. This directly addresses the cultural and environmental factors, as described by Otte, which have restricted the adoption of solar cooking.

1.2 Heat Storage Systems

Useful energy for solar cooking can be stored as sensible energy, as latent energy by means of a phase change, through a reversible chemical reaction, or through a combination of the three. Operating in the sensible temperature range of a material can be a low-cost option and easily accessible, but typically there is a lower energy density and the temperature is continuously decreasing during the discharge of the system. Storing latent energy through a phase change provides a fixed temperature as the material transitions from either a solid:solid, solid:liquid, or liquid:gas phase transition. By utilizing latent energy storage, a higher energy density can be achieved and it can produce a more familiar cooking experience by providing a stable temperature range. Chemical storage systems rely on a chemical reaction, often the hydration and dehydration of different materials. These systems don't suffer thermal losses during storage and can provide a long term thermal storage solution. Unfortunately they have much greater complexities in their system design and require either a working fluid or direct contact with the food. Limited work is available on chemical storage systems and fundamental material science research needs to occur before its potential for high temperature applications can be evaluated. This review will focus on select sensible and latent heat storage systems.

1.2.1 Sensible Heat Storage Systems

Sensible heat storage systems have been incorporated into several solar cooker designs. Many of these systems demonstrate a viable method to keep food warm and potentially heat food in the evening. Ramadan et al. created a simple and low cost, $15, box cooker that stored solar energy in sand. The authors claim to have achieved three hours of indoor cooking. This was achieved by heating .5 - .8 L of water in a container insulated with a reported .5 cm of sand (estimated to weigh .5 kg). The water and the sand were heated outside and brought inside where the sand was reported to have helped maintain the water temperature by acting as an insulator and as heat storage [16].

Haraksingh et al. demonstrated a passive, flat-plate collection system that stored solar thermal energy in coconut oil. Energy was transferred through a thermosyphon loop to two cooking pots immersed in the coconut oil. The system had a peak temperature of 150 °C and contained 5 MJ of energy when charged. The system was used to maintain water at the boiling point into the evening. They claimed to be able to cook very rapidly, boiling rice or sweet potatoes in 2 L of water in 20-25 minutes. They note on colder days, there was a 40 °C difference between their oil temperature and the cooking temperature achieved. No information was provided on additional cooking methods, only boiling was described [17].

Heetkamp utilized air as a heat transfer medium, a 4 m^2 parabolic concentrator, and rocks to obtain storage temperatures up to 400 °C. A metal wire brush was used to dissipate the large amount of energy collected by the parabolic concentrator and to transfer the energy to the air. The author filled a 210 L oil drum with rocks and insulated around the perimeter with 10 cm of rockwool insulation. The author estimated the system should have 11 kilowatt-hours of useful cooking energy when the rock bed cooled from 300 to 200 °C over a 5 hour period, but this was not demonstrated. The system was estimated to store over 100 MJ of energy and have a peak temperature of 400 °C. Unfortunately the author had difficulty recovering this energy at a high temperature. During discharge, Heetkamp reported air temperatures under 60 °C for the first three hours and reaching 100 °C after five hours. The author's final conclusion was the system should be used in a hybrid configuration, citing the low output temperatures the system achieved. Heetkamp implied you could reduce the fuel used by preheating the air in a conventional cooking system with this solar system. [18].

Schwarzer and Vieira da Silva demonstrated a scalable, flat panel system that stored thermal energy in vegetable oil and transferred it through pipes to the cooking surface using a thermal siphoning setup. Over 250 systems were built across India, Mali, Burkina Faso, South Africa, and in South and Central America. The systems varied in size from 1 to 12 m^2 of collector area with cooking areas sized for 5 - 100 L pots. A fully charged system could boil 5 L of water in 10 - 12 minutes [19, 20]. The authors believed the systems were best suited for large installations because of the cost and the need for financial assistance. A report from the Deutsche Geseelschaft für Technische Zusammenarbeit (GTZ) described several issues at the Tiger Kloof School in Vryburg, South Africa where one of the systems was installed. The report cited improperly sized thermal storage, distance from the kitchen, and lack of motivation for the staff as reasons it was only occasionally used for cooking and ultimately abandoned. The staff disliked having to travel outside to cook and they still had to use their traditional kitchens because the system was not properly sized. [21].

The Barli Development Institute for Rural Women adopted the use of Scheffler solar concentrators in the late 1990s. Scheffler concentrators have a fixed focal position. This design choice allows the solar cook to remain inside while an automated tracking system adjusts the solar concentrator and directs the solar energy to a fixed location. The Barli Institute soon realized that they needed to be able to use their solar system to cook when the sun was no longer available. In 2000, Deepak Gadhia and Wolfgang Scheffler upgraded their system with a sensible heat thermal storage solution [22]. Gadhia and Scheffler utilized a 400 kg cylinder of mild steel to store the energy collected from a 9.4 m^2 Scheffler, figure 1.5. In January 2017, the storage system was no longer in use due to a lack of maintenance. A former user reported that it was very useful for cooking, but it was very

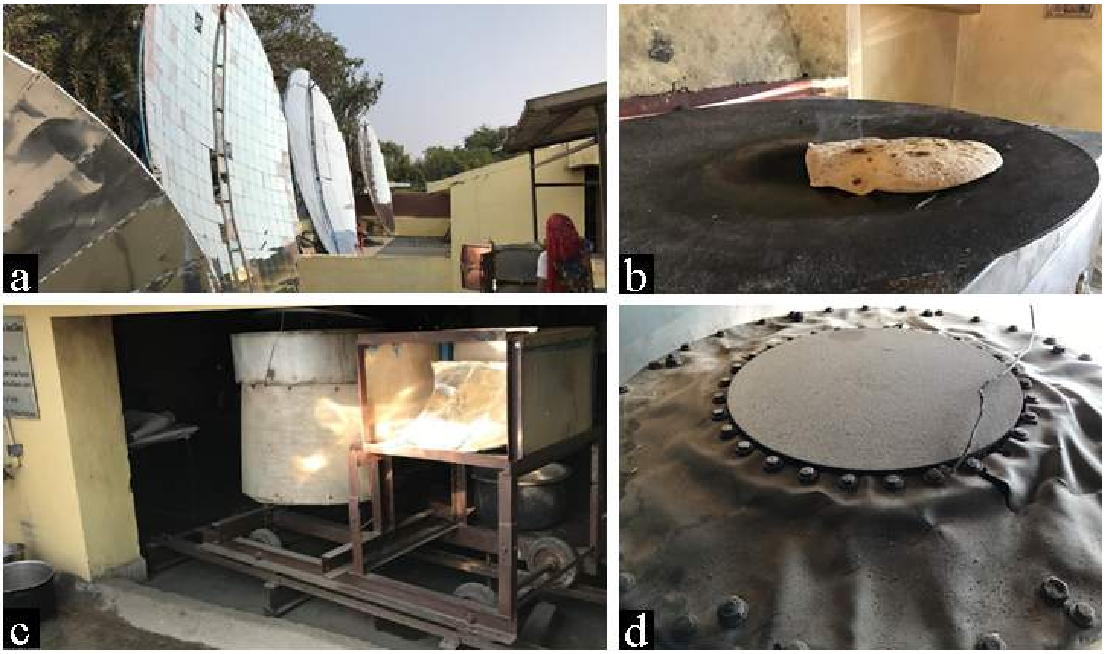

Figure 1.5: Photos of the solar cooking system at the Barli Development Institute for Rural Women in the Indian state of Madhya Pradesh. (a) Scheffler solar concentrators that are used to heat the storage system and for direct cooking. (b) Roti being cooked on a solar heated surface. (c) The thermal storage system and a direct cooking system on a railroad track. (d) The cooking surface of the storage system and a metal covering for the insulation. The thermal storage system is a 400 kg mild steel cylinder, surrounded by 8" of glass wool insulation.

difficult to physically switch the system from solar heating to storage due to its size and weight.

The above work illustrates that sensible heat storage systems have been used successfully to cook food. However, very limited research is available detailing how energy is recovered and instead focused on how much energy was potentially contained in the system. Systems that forced users to cook outside or were cumbersome to use saw limited long term use. The work by Heetkamp demonstrates that high temperature storage has limited use when it is not coupled with an appropriate heat transfer system. In addition, work needs to be done to emulate actual cooking - including selecting storage temperatures and materials to allow rapid cooking. The performance of the systems should be evaluated on how much energy can be recovered for cooking and at what rate.

1.2.2 Latent Heat Storage Systems

Latent heat storage systems were initially used as an add-on to traditional solar box cookers. Vessels containing a low temperature phase change material, ~100 °C, were added as an insert to existing solar cookers. The vessel could be used for temperature regulation, to increase the time that the box cooker kept food warm, or to cook when the sun was no longer available. Low temperature storage systems provide an acceptable option for users who live in areas with limited direct sunlight and who typically boil or slow roast their food. They have previously been reviewed by Cuce and Cuce [15]. An example was reviewed below.

Bushnell and later, Bushnell and Sohi, created an oven that contained a solid-solid phase change material, pentaerythritol. The oven was designed to be charged with concentrated solar thermal energy that would be circulated through the oven with a heat transfer oil. In the study, it was heated with an electric resistance heater. The authors reported the system efficiency and how long the system could remain hot. The cooking performance was not reported. The oven stored ~8 MJ of energy [23, 24].

Additional studies have been conducted using portable systems that store energy near the boiling point of water (Lecuona, Ramadan, Buddhi, Nandwani, and Sharma), higher temperature stationary systems (Okello, Mussard, and Tesfay), and higher temperature portable systems (Foong, Veremachi). These systems resemble the goals of the proposed system but tried to achieve them in various ways.

Lecuona et al. created a portable system for use with a parabolic concentrator [25]. They used two concentric cooking pots, where they stored phase change material in the outside pot and cooked in the interior pot. The pot was supported at the focal point of the parabolic dish as it was heated by the sun. After heating, the vessel was placed inside an insulated storage container that was kept inside the home. This cooker was designed to operate in the 100 °C range and was tested with two phase change materials, paraffin wax and erythritol. The vessel, without water, weighed 8.7 and 11.1 kg and required 1 MJ and 2.8 MJ of energy to fully melt the paraffin and the erythritol respectively. The total charging time from ambient temperature was not reported. In their follow up paper, the device was heated with water and the authors reported they could keep the food above 70 °C for up to 30 hours [26].

Stationary cooking systems have been designed to be either located outside the home or transfer the energy from outside into the home. The Norwegian University of Science and Technology (NTNU) created several stationary systems designed to charge a $KNO_3/NaNO_3$ mixture including an air-pebble bed system, a parabolic trough with a thermal siphoning oil loop, and a parabolic dish that utilizes a steam loop. These systems track the sun and do not require intervention by the user. The systems have charging times between 4 and 5 hours. When fully charged the air system took over 32 minutes to fry an egg and the oil system took 38 minutes to boil a liter of water [27–29].

NTNU has also demonstrated a portable system using the same $KNO_3/NaNO_3$ mixture as the stationary systems. Foong reported on the design and modeling of an unsealed heat storage system. It used .5 kg of the mixture and was charged to 230 - 260 °C in 2 - 2.5 hours [30, 31]. Foong used a single flat copper fin to transfer heat to the cooking surface. Continuing on this work, Veremachi increased the mass of the energy storage mixture to 7.5 kg. This increased the heating time of the system to about 4 hours. They calculated 5 MJ of the 38 MJ of available solar energy was collected and stored in the system, for a collection efficiency of 13%. No discharge or cooking performance data were reported so it is unclear how much of this energy would be recoverable for cooking [32, 33].

Research on solar thermal energy storage for cooking applications is under active development. The latent heat systems described above, [25, 26, 28, 30, 31, 33, 34], and one sensible heat system, [19, 20], are pictured in figure 1.6. It is clear there is not a consensus on approach and there is a need to improve cooking performance. Also, there is not a defined standard for reporting information to compare systems and measure improvements. This makes it difficult to evaluate the performance of the above systems. Section 3.3 outlines one approach to measure the system performance and provide an indication to users how the system will perform the most basic of cooking operations.

Figure 1.6: Recent stored solar thermal energy designs. Lecuona et al. has demonstrated a cooking pot with phase change materials that can be brought inside and stored [25, 26]. Schwarzer and Vieira da Silva created a stationary system with a large storage capacity [19, 20]. Foong et al. and Veremachi et al. developed and improved an unsealed, portable solar thermal energy device [30, 31, 33]. Mussard et al. developed a system that transferred and stored solar thermal energy indoors [28, 34]

1.3 Material Selection

A wide variety of materials have been reviewed for their suitability for thermal energy storage. Early research, as identified in sections 1.2.1 and 1.2.2, focused on materials that could be used in a temperature range from above the pasteurization point (63 °C) to around 250 °C [35]. Material selection in this work focused on materials that can operate in the 300 - 400 °C range. The expectation was that the higher temperatures would provide greater thermal storage potential and the higher heat transfer rates needed to spur adoption of solar technology as identified in the interviews. Experimentally, this range has not been explored in the literature, but Kenisarin reviewed the potential of thermal heat storage materials up to 1000 °C [36]. From this work, several chloride, hydroxide, and nitrate options were identified in the desired range. These materials were evaluated based on their safety, material compatibility, and material cost.

A selection of materials are listed in table 1.1, they represent a cross section of materials that could operate at high temperatures, have high heat capacities or latent heat of fusion values, or are metals. The table estimates the energy contained in the materials when heated from 25 °C to the indicated end point. The starting point of 25 °C was used to show the amount of energy that could be stored in the material above ambient temperature. While we are mainly focused on cooking, it may be useful to see how much energy is left over for additional tasks. This table was built using calculations based on values collected in the literature. Many of the materials referenced have not been evaluated in several decades and their source materials were not always available. In many cases, there were discrepancies in the data and therefore this table was only used to understand trends and the impacts of the different conditions. Kuravi et al. observed similar discrepancies when reporting on their concentrated solar thermal power plant experiments [37].

There are a few key points that were identified for comparison in table 1.1. The maximum operating point (MOP) was defined as either the boiling point of the material or 400 °C. An MOP of 401 °C was used to indicate materials that can operate above this temperature. The boiling point of the material also represents a key target threshold as a large amount of energy can be stored in the phase change. Section 4.3 explores these materials further and how candidate materials were evaluated. In addition, both the weight and the volume of the vessel are important considerations for the user and therefore the thermal energy densities were calculated for both conditions.

Table 1.1: Expected energy stored from 25 °C to the melting point or the maximum operating point (MOP). Materials are ranked based on the total energy density at the MOP.

			To Melting Point		To Max Operating Point	
	Melting Point (C)	Max Operating (C)	Total Energy Density (kj/kg)	Total Energy Density (MJ/m3)	Total Energy Density (kj/kg)	Total Energy Density (MJ/m3)
$NaNO_3$	307	380	712	1610	845	1910
$MgCl_2$/KCl/NaCl (37/20.5/42.5)	385	401	756	1360	771	1388
$MgCl_2$/KCl/NaCl (60/20.4/19.6)	380	401	741	1333	761	1370
Erythritol	118	330	468	678	761	1103
Lithium Nitrate	255	401	581	1382	716	1704
KNO_3	335	400	523	1104	535	1129
$NaNO_3$/KNO_3 (60:40)	220	401	375	674	592	1065
NaOH NaCl (80/20)	370	401	543	1159	558	1192
Aluminum	660	401	320	865	472	1275
Pentaerythritol	185	276	409	573	469	657
Stainless Steel (316)	1400	401	128	1023	188	1509
Iron	1538	401	116	919	171	1355

KNO_3 and $NaNO_3$ were selected for initial studies in this work because of their wide availability, simple chemistry, and low cost. In addition, they had been previously studied for concentrated solar power plant applications [38, 39]. While $NaNO_3$ had a higher total energy density, initially KNO_3 was believed to have a higher amount of energy stored in the phase change and it was selected for testing in chapter 3. Pentaerythritol was eliminated for its low energy storage capacity. Erythritol has been shown to degrade through cycling and was eliminated in favor of materials with long term stability. Lithium nitrate was expected to perform similar to sodium nitrate and was expected to have a high cost with limited availability. It was excluded in favor of sodium nitrate.

2 Research Objectives and Initial Work

2.1 Objectives

This work began with the premise that in order for solar thermal cooking to be successfully adopted, the user's experience needed to be similar to their current cooking practice. For the vast majority of potential users, that involves cooking at a high temperature and power (i.e., rate of energy transfer), when and where they want. In contrast, solar energy is naturally available at a low power and requires additional manipulation to make it useful for cooking. The goal of this research is to make solar energy useful for cooking by storing the thermal energy in a portable fashion and exploring what materials allow it to be recovered at an acceptable power level. The specific contributions of this work include:

1. Development of a sealed, portable solar thermal energy vessel
2. Measurement of the performance of the proposed system
3. Testing the performance of candidate materials, that operate in the 300 - 400 °C range, using the proposed storage vessel

By satisfying these objectives, it is expected that potential users will have a portable solar thermal energy system and a range of material options that they can evaluate and match with their personal cooking style.

2.2 Cooking with Thermal Energy Storage Materials

2.2.1 Introduction

The purpose of this study was to verify that a device using thermal energy storage materials can cook food similar to traditional fuels. The objective of this test was to show we could bake, fry, and sear common foods with an energy storage material that operates in the defined range of 300-400 °C.

2.2.2 Materials and Methods

A basic cooking configuration was created using an insulated kamado style grill, $NaNO_3$, and a cooking pot. The setup is shown in figure 2.1. $NaNO_3$ was selected for its energy storage capacity, low cost, and availability. $NaNO_3$ prills were melted in an aluminum container using a hot plate. The molten salt and containment vessel were then placed inside a kamado grill. A 6 quart cast iron cooking pot was then partially submerged into the molten salt. The cooking chamber was then closed to allow the chamber and cooking pot to increase in temperature. The cooking chamber was kept closed during cooking and lids were used to minimize heat loss in the system. Baking tests were conducted by using a grill grate to elevate the food off the cooking surface and the lid of the grill was kept closed.

The $NaNO_3$ was fully melted before the test and if the food was cooked it was considered a success. This was useful to prove the system could accomplish common cooking tasks like baking, frying, and boiling. Caloric information was obtained from www.nutrition.gov.

2.2.3 Results

Muffins, hamburger patties, and rice were cooked in separate experiments to demonstrate the common cooking tasks independently. In addition, a meal for several people was prepared. Steak, pork, onion, and rice were cooked in succession, totaling 3300 food calories. The steak was seared on both sides by placing it directly on the cooking surface and then a small grill grate was added to reduce the heat and allow it to finish cooking. The total cooking time was approximately 14 minutes and it was cooked to a well done state. The pork and onion were then added and fried for 20 minutes. The mixture was fully cooked and the pork was lightly charred. Finally, the rice and water were added. The rice was fully cooked in about 26 minutes. The total cooking time of the meal was 1 hour. All food items were cooked to a satisfactory level and exceeded minimum cooking standards. The meats had internal temperatures above recommended safe levels and the rice was cooked passed the point where it was soft throughout. While cooking times and styles differ, the times to cook each dish appear to be within commonly accepted estimates.

Figure 2.1: Cooking setup - an insulated kamado grill, a 6 quart aluminum pan with $NaNO_3$, and a 6 quart cast iron dutch oven.

2.2.4 Conclusions

This initial demonstration proved $NaNO_3$ could hold and transfer enough energy, at an appropriate temperature, to cook a significant quantity of food. The most common tasks of baking, frying, and boiling were demonstrated. The cooking times were similar to conventional methods. This evidence was sufficient to justify further study of $NaNO_3$ and similar materials. The next step was to determine under what conditions these materials could be heated with energy collected by the sun.

2.3 Solar Melting of KNO_3 and $NaNO_3$

2.3.1 Introduction

The main purpose of this study was to determine under what conditions high temperature thermal energy storage materials like KNO_3 and $NaNO_3$ could be melted with commercial parabolic concentrators and at what quantity.

2.3.2 Methods and Materials

Testing was conducted in Mosco, Colorado on October 24 - 27, 2014. This location was selected based on historical weather and solar insolation data and it was forecast to have clear skies during the testing period. Sodium nitrate and potassium nitrate were chosen as energy storage materials for their high temperature melting point, low cost, and global availability. Tests were conducted with 1.5 and 3 kg of KNO_3 and $NaNO_3$. In addition, containers with 4 kg of KNO_3 were also tested. Test vessels were prepared by melting the appropriate salt in an aluminum container with an electric hot plate. A spiral of aluminum flashing was added to a portion of the vessels to act as a heat transfer fin. The salt was allowed to cool to room temperature and the vessel bottoms were coated with black paint to enhance their ability to absorb solar radiation. The vessels were insulated on the top and sides with rockwool insulation. The setup is shown in figure 2.2. Solar irradiance data were collected using a pyranometer and recorded manually. Thermocouples were mounted in four quadrants near the top perimeter of the vessel using a layered structure of aluminum foil, as shown in figure 2.3. Data were collected using k-type thermocouples and a portable data logger. The material was assumed melted when the average of the quadrants was above the melting point of the material and the melt was verified by visual inspection.

Two commercially available, unmodified parabolic cookers were used to conduct the tests. The Solar Burner and the Sol Source were commercially available in the USA and had a contrasting set

Figure 2.2: Solar collection setup in Mosca, Colorado. The Sol Source from One Earth Designs is on the left and the Solar Burner from Cantina-West is on the right.

Figure 2.3: A four thermocouple configuration was used to determine if the vessel was melted. The bends created a spring type action and helped ensure the thermocouples contacted the salt temperature.

Figure 2.4: This is an example of a failed melt that occurred with the Sol Source.

Figure 2.5: This is an example of a successful melt as there are no solid salt pieces observed.

of properties. The Solar burner is a low-cost parabolic dish with a collection area of 1.5 m^2. It has a low quality reflective surface. The Sol Source has a collection area of approximately 1.1 m^2 but has a very high quality reflective coating. The geometry of the Sol Source allows it to tightly focus the solar radiation. The two dishes were compared side by side during the second day of tests.

2.3.3 Results and Discussion

Table 2.1 - 2.3 show the results of four days of testing. The Solar Burner was used to melt 1.5 kg of $NaNO_3$ and up to 4 kg of KNO_3. The Sol Source was used to melt up to 3 kg of $NaNO_3$. The direct comparison of the Sol Source and the Solar Burner is shown in table 2.3. The Solar Burner was able to melt two additional vessels, 3 kg, of $NaNO_3$ during a full day of testing.

The time of day appeared to have been a significant factor affecting the time to melt. This influenced both the available solar radiation and the amount incident on the vessel surface. In the morning, a portion of the solar radiation strikes the vessel insulation due to the angle of the sun. By solar noon, all of the solar radiation is incident on the vessel surface. The solar irradiance data were collected at the start and finish of each test. Only the initial value from each test is reported in table 2.1 and 2.2. Without periodic sampling of the solar irradiance, it is unclear if clouds interfered with any of the results.

The melt patterns observed with the Sol Source suggested a heat transfer system was necessary. The Sol Source achieved a full melt at the location of the focused beam without significant spreading, figure 2.4. In addition, during one test a hole was melted in the bottom of the aluminum vessel as shown in figure 2.6. The fins appeared to have improved the temperature distribution for the Sol Source and reduced its overall heating time. The fin results were inconclusive with the Solar Burner.

Table 2.1: Melting results with the Solar Burner parabolic concentrator.

Irradiance (W/m^2)	Material	Mass (kg)	Melt Time (min)	Notes
950	KNO3	1.5	60	
1050	KNO3	3	132	
850	KNO3	4	160	Early Morning
901	KNO3	4	167	Fins
1042	KNO3	4	114	High Winds - Peak Sun
1296	KNO3	4	-	Clouds and Wind
950	NaNO3	1.5	63	
950	NaNO3	1.5	44	No Fins
1000	NaNO3	1.5	53	No Fins
1050	NaNO3	1.5	47	Fins
1055	NaNO3	1.5	56	Fins
1080	NaNO3	1.5	51	Fins
1080	NaNO3	1.5	33	No Fins
1080	NaNO3	1.5	41	No Fins
1083	NaNO3	1.5	40	No Fins
1092	NaNO3	1.5	42	Fins

Table 2.2: $NaNO_3$ melting results with the Sol Source parabolic concentrator.

Irradiance (W/m^2)	Mass (kg)	Melt Time (min)	Notes
860	1.5	-	Plenum
924	1.5	-	Pot Melted
950	1.5	74	
950	1.5	87	No Fins
1000	1.5	150	No Fins, T Error
1026	1.5	83	No Fins, Plenum
1050	1.5	79	Fins
1069	1.5	-	
1080	1.5	69	Fins
1080	1.5	80	No Fins
1092	1.5	83	No Fins
1092	1.5	109	Fins
1050	3	181	

Table 2.3: Melting times for 1.5kg of $NaNO_3$ during a day-long side-by-side test of the Solar Burner and Sol Source.

Concentrator	Melt Time (min)	Test Conditions
Solar Burner	44	No Fins
Sol Source	87	
Solar Burner	47	Fins
Sol Source	79	
Solar Burner	33	No Fins
Sol Source	80	
Solar Burner	40	No Fins
Sol Source	83	
Solar Burner	42	Fins
Sol Source	109	
Solar Burner	41	No Fins
	56	

Figure 2.6: $NaNO_3$ leaked through this pan. It was damaged by the tightly focused beam of solar energy created by the Sol Source parabolic cooker.

2.3.4 Conclusions

KNO_3 and $NaNO_3$ were melted using commercially available parabolic cookers. It was demonstrated that up to 3 kg of $NaNO_3$ and up to 4 kg of KNO_3 could be melted in 2 - 3 hours. Several vessels could be melted in a single day. Future studies will favor concentrators with a large concentration area, like the Solar Burner. In addition, the vessel will be designed to distribute the energy from concentrated beams and transfer it evenly through the energy storage material. In future tests, solar irradiance values will be collected at regular intervals so the average energy incident on the dish during an experiment can be calculated and used to compare experiments.

3 KNO_3 Solar Heating and Recovery Testing

3.1 Introduction

The previous tests proved that it was possible to cook on and melt energy storage materials that operate in the 300 - 400 °C range. This study quantifies the performance of a stored solar thermal energy system using unmodified parabolic dishes. Tests measured (a) time-temperature relationships during solar heating of a vessel containing KNO_3 up to temperatures of 300 - 400 °C (570 - 750 °F) and (b) recovery of energy from the storage vessel using a water heating test. A water heating test was chosen to provide an indication of performance that is connected to a common cooking task, boiling.

3.2 Vessel Design and Fabrication

The energy storage vessel was designed with a focus on using commercially available components or simply geometries. COMSOL modeling was used to determine appropriate fin thickness and spacing considerations. The vessel was composed of: the heat transfer unit (1 plate and 2 concentric tubes), the energy storage material and its container, and insulation. The heat transfer plate was cut with an abrasive water jet machine from a sheet of 6061 aluminum to create a solid cylinder with a diameter of 8.5 inches and a depth of .25 inches. The 6 and 3 inch concentric tubes were welded onto the heat transfer plate and then the unit was welded to the aluminum containment vessel. A hole was drilled into the heat transfer plate and the energy storage material, KNO_3, was added. The vessel was heated in an oven at 375 °C. Additional KNO_3 was added until the total amount was equal to 5 kg. An attempt was made to seal the vessels with aluminum pipe plugs, but they proved to be insufficient during solar heating and leaked molten salt. To insert the plug, the furnace was heated to 425 °C for 15 minutes and the aluminum plug was inserted into the plate.

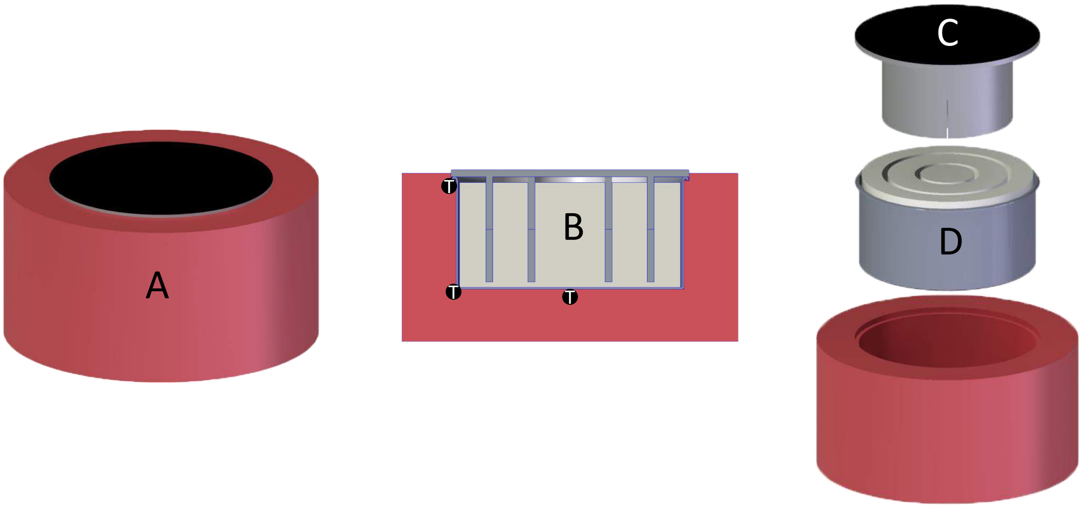

Figure 3.1: External, cross section, and exploded view of the storage system. The 4 main system components are labeled: (A) Pyrogel XT-E (B) Thermal storage material, KNO_3 (C) 6061 Aluminum plate and tubes (D) Aluminum container. Three thermocouples (T) in the cross section view are referenced as the plate, side, and center thermocouples.

Once the vessel was cooled, K-type thermocouples were attached with thermocouple cement at the locations indicated in figure 3.1 in the cross section view. The vessel was then wrapped on the sides and bottom with 50 mm of Pyrogel insulation. An outer covering of aluminum foil was used to reduce convection losses through any gaps in the insulation and to mitigate the dust generated by disturbing the insulation.

A coating was applied to the exposed surface of the vessel to enhance the solar absorption. Either BBQ paint or Sol-Kote was applied per the manufacturer's directions. Sol-Kote is designed to have a lower emissivity (.5) than absorptivity (.95) and therefore emit less radiation. The BBQ grill paint has the same emissivity and absorptivity (.98).

3.3 Methods

The testing site for this study was chosen based on data from solar insolation maps and weather forecasts. Nashville, Tennessee was selected as it was expected to have several days of sunshine and historically has higher solar insolation than similar areas with expected sunshine. The tests were carried out from October 5th - 7th, 2015. Three 1.5 m^2 parabolic solar cookers were set up as recommended by the manufacturer. The parabolic concentrators were unmodified and spaced

Figure 3.2: Experimental setup for the solar heating tests.

sufficiently apart so that they would not cast a shadow on each other during the duration of a test. A picture of the setup is shown in figure 3.2. Twelve vessels were fabricated as described in section 3.2 and individually numbered. Four thermocouples were connected to a portable datalogger to record temperature data during charging. Three thermocouples were cemented to the vessel and one was used to measure ambient air temperature. Direct normal solar irradiance data and temperature readouts from the data loggers were recorded manually by the user every 15 minutes during testing. The energy storage material contained within the vessel was considered completely melted and the vessel "charged" when the vessel's center thermocouple reached 340 °C, ~5°C above the material melting point. The vessel was then removed from the parabolic cooker and the thermocouples were transferred to a separate data acquisition system for water boil tests. Three thermocouples from the vessel and an additional K-type thermocouple for the water were used to record the temperature of the system as it heated successive 1 L volumes of water from ambient temperature to 95 °C. At 95 °C, the water was removed and replaced with fresh water. The test was concluded when the water temperature failed to reach 95 °C and began to decline. 95 °C was chosen to approximate a full boil while limiting the amount of energy lost due to water vaporization.

Figure 3.3, provides a graphical description of how energy was transferred by the system during energy collection and recovery. Figure 3.4, provides an estimate of the magnitude of these transfers for the system described in this paper. The solar irradiance and water boil test data were used to calculate the efficiency of the stored solar thermal energy system. The efficiency of the system was calculated as follows:

$$\text{System Efficiency} = \frac{\text{Energy Recovered}}{\text{Available Solar Radiation}} \tag{3.1}$$

where the available solar radiation in megajoules (MJ) was calculated from the solar irradiance data and represents the amount of sun shining over the area of the dish while the vessel was charging.

$$\text{Available Solar Radiation} = (\text{Radiation}_1 * t_1 + \ldots + \text{Radiation}_n * \text{t}_n) * \text{A}_{dish} \tag{3.2}$$

where the solar irradiation measurement (Radiation_n) is in MW/m^2, the time t_n is in seconds, and the A_{dish} is in m^2. This value provides an estimate for the maximum amount of solar radiation that could have been collected, rather than the actual amount of solar radiation concentrated and collected into the vessel. This provides a fair means to compare systems with more efficient charging mechanisms such as highly reflective coatings, smaller vessels, and better concentration schemes.

The energy recovered was calculated by equation 3.3:

$$\text{Energy Recovered} = (m_{water_1} * \Delta T_1 + \ldots + m_{water_n} * \Delta T_n) * C_{p_{water}} \tag{3.3}$$

where ΔT_i is the change in water temperature for each successive liter of water, m_{water_i} is the mass of water for each test (1 kg), and $\text{C}_{p_{water}}$ is the heat capacity of water (4.184 J/g°C). The final heating attempt was included in equation 3.3 whether it reached 95 °C or not.

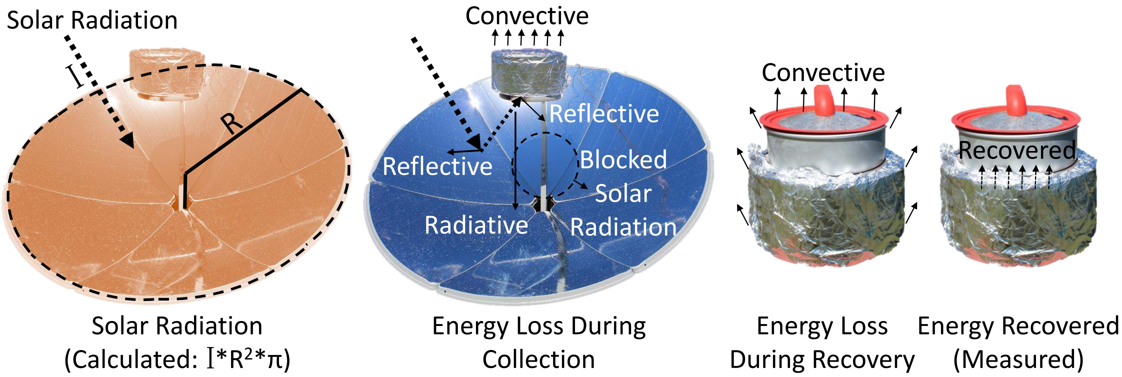

Solar Radiation (Calculated: $I*R^2*\pi$)

Energy Loss During Collection

Energy Loss During Recovery

Energy Recovered (Measured)

Figure 3.3: The efficiency of the system was measured by the total amount of energy recovered in the water heated in the water boil tests divided by the total available solar radiation. This figure notes where energy is being lost in this process.

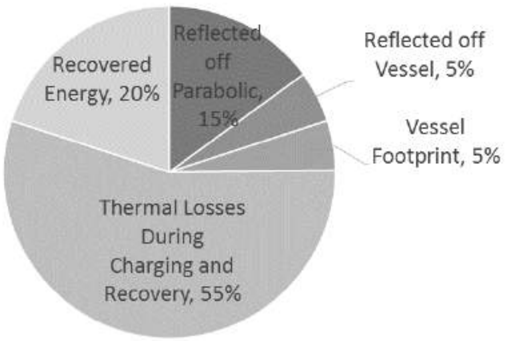

Figure 3.4: Approximate distribution of the total available solar radiation incident on the dish.

3.4 Results

Over the course of three days, 26 attempts were made to charge the KNO_3 vessels. Four of the experiments were excluded because the tests was ended before the vessel reached 340 °C; insufficient personnel time was available to complete these experiments. Two more were excluded because the vessels were removed from charging before reaching 340 °C to evaluate the test procedure.

3.4.1 Vessel Charging

The solar irradiance during charging averaged 958 W/m^2 with a minimum of 817 W/m^2 and a maximum of 1006 W/m^2. The 12 vessels were tested a total of 20 times and took an average of 141 minutes to charge. A representative temperature verse time graph during vessel charging is shown in figure 3.5. The thermal couple nearest to the charging surface, the plate thermocouple, heats up first and then all three thermocouples rise at a similar rate. At approximately 45 minutes into the test a leveling off of all three thermocouples can be observed as KNO_3 undergoes a solid-solid phase transition. At 150 minutes into the test, the plate temperature decreases because a large cloud blocked the sun and the top plate began cooling. In addition, the side and center thermocouples leveled off again as the KNO_3 completes a solid-liquid phase transition.

Unfortunately, many vessels leaked molten salt during testing. They leaked between 5 and 50 grams of KNO_3 during a single charge cycle. The aluminum plug became soft during fabrication and may have prevented adequate tightening, allowing salt to be discharged from the vessel. The vessel design and sealing process has since been modified and the vessels no longer leak. This process is described in section 4.2.

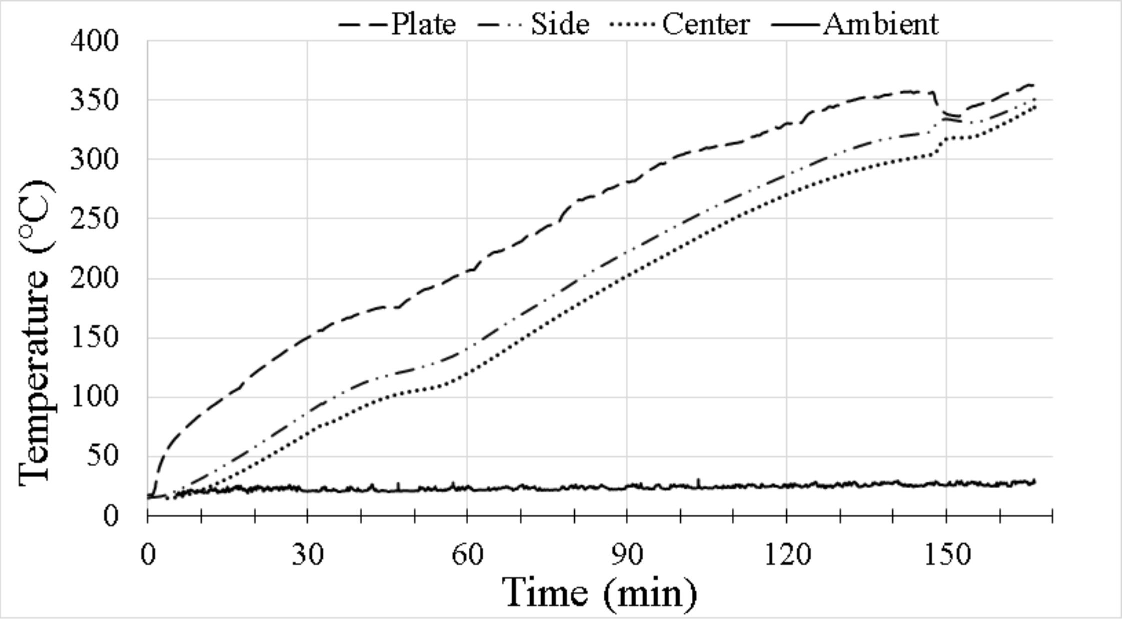

Figure 3.5: Sample output data from vessel charging. Vessel was charged on October 7th, 2015 from 8:30 am to 11:15 am.

3.4.2 Energy Recovery

Overall, an average of 2.3 MJ of energy was recovered from each vessel, boiling 7 - 8 L of water. This neglected any energy lost due to evaporation and the remaining energy in the vessel. The total energy stored, from 340 C to 25 C, was calculated to be 3.1 MJ. Table 3.1 shows the average time for the first 5 L of water to go from ambient temperature to 95 °C for the 20 completed tests. After 5 L, vessel performance was less predictable and dependent on the specific charging conditions for that vessel. Table 3.2 lists the average power level of the 20 tests for each individual liter of water boiled and the 5 L summary. Figure 3.6 shows an example of the temperature characteristics of the vessel during a recovery test. While the vessel was removed when the center thermocouple reached 343 °C, the vessel equilibrated at 350 °C. Since the initial temperature of the plate and side thermocouples were above 340 °C, this test would be expected to boil the average number of liters of water. If the plate and side thermocouple were much higher than the center thermocouple, it would be expected to boil an extra liter or two of water. In this case, 7 L of water were boiled and an 8th liter was heated to 93 °C.

The average system efficiency for the 20 tests conducted was 19%. For morning tests that began after 8 am and finished charging by 12 pm, the average system efficiency was 17.9%. For midday

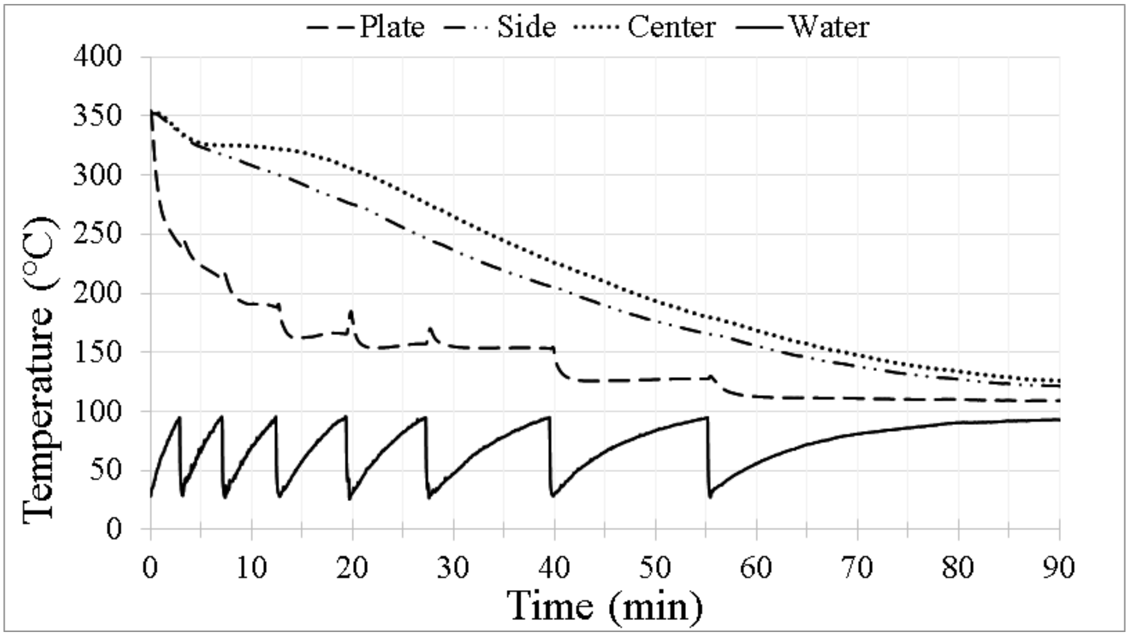

Figure 3.6: Sample output data from the water boil test. Seven liters of water were boiled with an eighth liter approaching 95 °C. Vessel was charged on October 7th, 2015 from 8:30 am to 11:15 am. This is the same vessel used in figure 3.5.

Table 3.1: Average time (mm:ss) to boil for each liter of water during vessel recovery.

	Liter					
	1st	2nd	3rd	4th	5th	5L Total
Average Time to Boil	3:33	4:19	5:54	7:23	8:21	29:31
Standard Deviation	1:14	1:31	1:34	1:20	1:30	6:18

Table 3.2: Average power (W) for each liter of water during vessel recovery.

	Liter					
	1st	2nd	3rd	4th	5th	5L Total
Average Power	1397	1152	843	660	576	816
Standard Deviation	369	266	219	109	102	151

tests that began after 11am and concluded by 2 pm, the average system efficiency was 21.6%. Using a Welch Two Sample t-test ($n_{morning}$=8, n_{midday}=7, t=-3.2882, df=10.519, p-value=0.007654), there was a significant difference between the two testing periods. This can be expected as solar irradiation values were increasing between these two time periods and the parabolic dishes direct more energy to the charging surface when the sun is higher in the sky.

Only the morning test had enough samples to compare the performance of the surface coatings. The average efficiency was 19.5% and 16.9% for the Sol-Kote and BBQ paint respectively. Using a Welch Two Sample t-test (n_{bbq}=5, n_{sol}=3, t=-3.7894, df=4.315, p-value=0.01678), the Sol-Kote coating had a significant impact on the system efficiency. Similar improvements were observed for charging time and system efficiency in general, but the significance could not be confirmed using statistical analysis.

3.5 Conclusions

Solar thermal energy can be collected in portable vessels and used to boil and heat several liters of water. The vessels, containing 5 kg of KNO_3, were charged using commercially available parabolic solar cookers in about 141 minutes and at their peak charge, boiled 7 - 8 L of water. The average power output of the vessel for the first 5 L was ~800 W. The vessels were used to recover 2.3 MJ of energy in a useful manner, with an average efficiency of 19%. The results are promising for the development of stored solar thermal energy systems for cooking and other small-scale uses of thermal energy, including space heating, grain drying and other types of food processing, charging electronics and lighting. Further work is expected to improve solar charging time, to improve system efficiency, and to study its acceptability to users.

4 Measuring the Energy Recovered from Solar Thermal Energy Storage Materials

4.1 Introduction

The purpose of this study is to experimentally compare the performance of candidate thermal energy storage materials and determine the important characteristics to consider when selecting a material for a portable vessel. Several materials were reviewed and their theoretical energy storage capabilities were calculated. Five candidate materials were selected and test vessels were fabricated containing the candidate materials. An energy recovery test was conducted on these candidate materials and used to evaluate and compare them.

4.2 Vessel Fabrication

The vessel fabrication process described in section 3.2 was updated to prevent leaks. Previously, salt could become trapped in the plug threads and prevent it from sealing. Having a closed vessel extends the utility of the device as it can then be used in any orientation and with hygroscopic materials. The vessel was composed of: the heat transfer plate and 2 concentric tubes to act as heat transfer fins, the energy storage material and container, the insulation, and an outer shell with handles. The heat transfer plate was cut with a water jet from a sheet of 6061 aluminum to create a solid cylinder with a diameter of 8.5 inches and a depth of .25 inches. The fins were made from 6 and 3 inch ID 6061 aluminum with .25 inch walls and were cut to 3.75 inch lengths. A .0625 inch slot was cut at a depth of 1.875 inches from the top and the bottom in each of the concentric tubes, 180 degrees apart as shown in figure 4.1. The concentric tubes were centered and welded to the heat transfer plate. The slot creates a channel for air to escape when the assembly is inserted into molten thermal storage material. The thermal storage material was melted inside the containment vessel and then the heat transfer assembly was lowered into the molten material. This assembly was then welded, at room temperature, around the perimeter of the heat transfer plate to seal the vessel. A .0625 inch diameter vent hole was then drilled into the weld and it was reheated to the maximum operating point (the material boiling point or above 401 °C) and rewelded to seal the vessel before cooling. This was done to prevent the vessel from deforming under normal heating cycles and reduce any risk of over-pressurizing the vessel. The heat transfer plate was coated with Sol-Kote and baked at 200 °C per the manufacturer's recommendations. Two k-type thermocouples were secured to the bottom center of the containment vessel with thermocouple cement. The vessel was then wrapped in insulation and an outer shell was secured around the vessel. The complete assembly is shown in figure 4.2. This process produced vessels that maintained salt containment and did not leak when maintained below the maximum operating temperature.

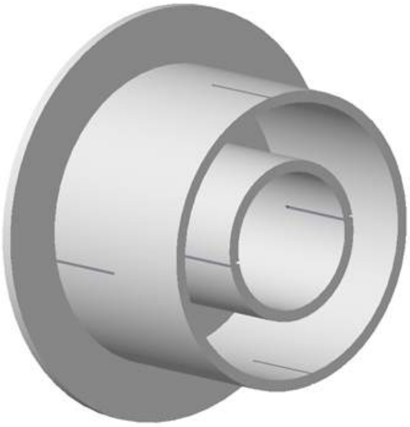

Figure 4.1: Slots are cut into the heat transfer surface to allow fluid movement during construction.

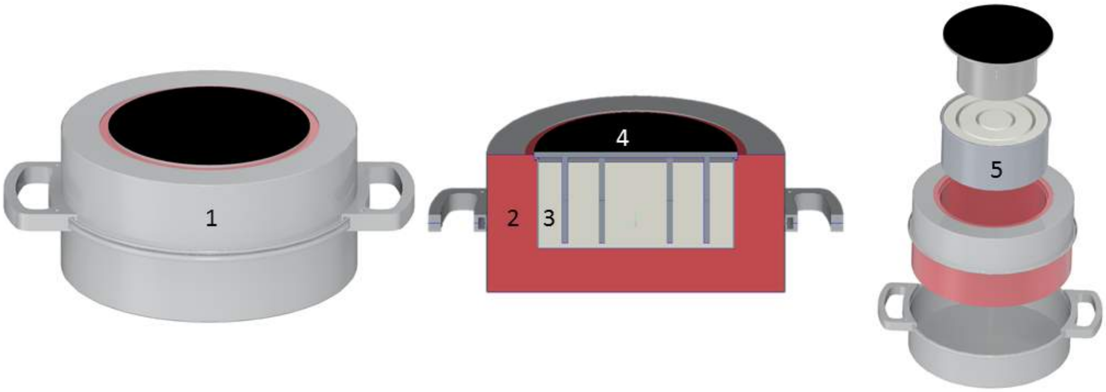

Figure 4.2: External, cross section, and exploded view of the storage system. 1: Two 12" x 3" Aluminum containers 2: Pyrogel XT-E, 3: Thermal storage material (TSM) 4: 6061 Aluminum plate and tubes 5: 8" x 4"Aluminum TSM container

4.3 Materials and Methods

4.3.1 Review of Candidate Materials

A search for candidate materials began by looking for materials that can operate in the 300 - 400 °C range. This range was selected based on the goal of emulating fire and the positive results discussed in section 2.2 and chapter 3. Section 1.3 reviewed several heat storage systems and materials, section 1.3 specifically covered high temperature materials, from these reviews four candidate latent heat storage materials were selected and one sensible heat storage material.

Since KNO_3 was previous studied in section 3, it was included as a candidate material. While technical data was not previously collected, $NaNO_3$ was also included due to its cooking performance in section 2.2. KNO_3 and $NaNO_3$ are common materials used throughout the world as fertilizers and are available at a low cost, under $1 USD/kg. $NaNO_3$ has a similar operating range as KNO_3 and both are considered chemically stable until 450 °C, at which point there is a higher probability of a reversible nitrate to nitrite reaction [39].

A mixture of KNO_3 and $NaNO_3$ is used in concentrated solar thermal power plants as a thermal transport fluid and NTNU uses it in their solar thermal storage research systems. It has a significant advantage in a sealed system, as it boils at a much higher temperature than either component independently. Its phase change is in the 200 - 300 °C range depending on the composition, allowing a comparison of a material with a lower phase change temperature that can be tested up to the same operating temperatures as KNO_3 and $NaNO_3$. The mixture chosen for this study, (60/40 mol%) $NaNO_3/KNO_3$, has a melting point at ~235 °C.

Hygroscopic materials are very difficult to work with and must be kept dry to maintain the integrity of the material. Two high potential hygroscopic materials were identified that operated in the 300 - 400 °C range and have a latent energy of ~370 - 400 kj/kg [40]. Early testing with an (80/20) mixture of NaOH and NaCl, demonstrated the difficulty in using hydroscopic materials. This mixture was excluded because it is incompatible with the aluminum containment system described in section 4.2 and a material with similar characteristics was available. The similar material, a mixture of $MgCl_2$ KCl NaCl (37/20.5/42.5 wt%) is compatible with the vessel described in this work. This mixture operates at the high limit of our desired temperature range, having a melting point between 380 - 400 °C and was reported to store a significant amount of energy in the phase change, ~400 kj/kg. The mixture was selected because it has the highest latent energy and the lowest heat capacity out of the four candidate materials. These chlorides have a low cost and do not have the regulatory restrictions that apply to oxidizers like KNO_3 and $NaNO_3$.

In addition to the four latent heat storage materials, a vessel containing a solid aluminum cylinder was created. While using a machined or extruded aluminum cylinder would probably be prohibitively expensive from a commercial standpoint, a cast part of aluminum could be fabricated in bulk for around \$4 USD/kg. Depending on the manufacturing costs of the latent heat systems, this could be cost competitive. The cylinder available for testing had a comparable volume to the test vessels, 3.1 compared to 3.2 dm^3. The cylinder weighed 8.7 kg, while each latent system weighed 7 kg when the aluminum heat transfer and containment vessel are included.

4.3.2 Theoretical Energy Storage Calculations

The following tables report how much energy can be stored in the candidate materials and select material alternatives. Several heating options are reviewed since there are different contexts under which a thermal heat storage material may be evaluated. The material melting point and the maximum operating point (MOP) were selected as the upper limits for heating.

The estimated energy stored from 25 °C to the melting point has been calculated in table 4.1 and in table 4.2 for the MOP. $NaNO_3$ has the highest heat capacity in the solid state of this group, consequentially it has the highest energy stored through the phase change. Erythritol and $LiNO_3$ have very high heat capacity values in the liquid phase and outperform many of the other materials when taken to the MOP. Even though pentaerytritol stores a significant amount of energy in the phase change, its low heat capacity and temperature range make it a low performer for this application. This test case demonstrates that it is advantageous to use a material with a high heat capacity, particularly in the liquid phase, and operate at a high temperature.

At the conclusion of the water boil tests described in chapter 3, the last boil occurred at ~115 °C. This was then used as an expected endpoint to calculate how much energy would be available to boil water. The materials were re-evaluated and ranked, this time considering expected water boil performance. The results are displayed in table 4.3, up to the material boiling point, and table 4.4, up to the maximum operating temperature. Overall the trends are similar. The relative performance of $NaNO_3$ is lower compared to Erythritol and $LiNO_3$, again due to their heat capacity in the liquid phase. These energy calculations were created using static heat capacities and these results show it could be advantageous to use temperature dependent values to build a more accurate model. Unfortunately, there is variability in the reported measurements and limited availability for some materials so it may not have improved these estimates. KNO_3 stayed in the bottom half of expected performance in all four tables. A conservative value of 100 kj/kg was used for its latent heat of fusion, the reported values in the literature ranged from 90 to 260 kj/kg.

The results from tables 4.1 - 4.4 did not justify the additional material costs, reactivity, and cycling risks associated with $LiNO_3$, Erythritol, and NaOH NaCl (80/20), as each material was comparable to one of the candidate materials; $NaNO_3$, $NaNO_3/KNO_3$ (60/40), and $MgCl_2$ KCl NaCl (37/20.5/42.5) respectively. Aluminum, KNO_3, $NaNO_3$, NaNO $3/KNO_3$ (60/40), and $MgCl_2$ KCl NaCl (37/20.5/42.5) were tested. The four candidate latent heat materials are ranked using the energy stored by volume in tables 4.1 - 4.4. Since comparing the materials experimentally by weight is more practical, the candidate materials have been reranked by weight, under the same conditions, in tables 4.5 - 4.8. The following study compared the materials by weight when heated to the MOP and measured the energy recovered with a water boil test.

Table 4.1: Candidate thermal energy storage materials ranked by highest total energy density (TED) by volume when heated from 25 °C to the melting point.

	Melting Point [°C]	TED - Weight (kj/kg)	TED - Volume (MJ/m^3)
$NaNO_3$	307	712	1610
$LiNO_3$	255	581	1382
$MgCl_2$ KCl NaCl (37/20.5/42.5)	385	756	1360
NaOH NaCl (80/20)	370	543	1159
KNO_3	335	523	1104
Erythritol	118	468	678
$NaNO_3$/KNO_3 (60/40)	220	375	674
Pentaerythritol	185	409	573

Table 4.2: Candidate thermal energy storage materials ranked by highest total energy density (TED) by volume when heated from 25 °C to the maximum operating temperature (boiling point or 401 °C).

	Operating Point [°C]	TED - Weight (kj/kg)	TED - Volume (MJ/m^3)
$LiNO_3$	401	878	2090
$NaNO_3$	380	849	1920
Erythritol	330	1054	1528
$MgCl_2$ KCl NaCl (37/20.5/42.5)	401	771	1388
$NaNO_3$/KNO_3 (60/40)	401	664	1196
NaOH NaCl (80/20)	401	558	1192
KNO_3	400	536	1132
Pentaerythritol	276	469	657

Table 4.3: Candidate thermal energy storage materials ranked by highest total energy density (TED) by volume when heated from 115 °C to the melting point.

	Melting Point [°C]	TED - Weight (kj/kg)	TED - Volume (MJ/m^3)
$NaNO_3$	307	548	1239
$MgCl_2$ KCl NaCl (37/20.5/42.5)	385	669	1205
$LiNO_3$	255	497	1183
NaOH NaCl (80/20)	370	498	1063
KNO_3	335	355	928
Erythritol	118	344	498
Pentaerythritol	185	349	489
$NaNO_3/KNO_3$ (60/40)	220	267	480

Table 4.4: Candidate thermal energy storage materials ranked by highest total energy density (TED) by volume when heated from 115 °C to the maximum operating temperature (boiling point or 401 °C).

	Operating Point [°C]	TED - Weight (kj/kg)	TED - Volume (MJ/m^3)
$LiNO_3$	401	795	1892
$NaNO_3$	380	686	1550
Erythritol	330	929	1348
$MgCl_2$ KCl NaCl (37/20.5/42.5)	401	685	1232
NaOH NaCl (80/20)	401	513	1096
$NaNO_3/KNO_3$ (60/40)	401	556	1001
KNO_3	400	440	928
Pentaerythritol	276	410	574

Table 4.5: Candidate thermal energy storage materials ranked by highest total energy density (TED) by weight when heated from 25 °C to the melting point.

	Melting Point [°C]	TED - Weight (kj/kg)	TED - Volume (MJ/m^3)
$MgCl_2$ KCl NaCl (37/20.5/42.5)	385	756	1360
$NaNO_3$	307	712	1610
KNO_3	335	523	1104
$NaNO_3/KNO_3$ (60/40)	220	375	674

Table 4.6: Candidate thermal energy storage materials ranked by highest total energy density (TED) by weight when heated from 25 °C to the maximum operating temperature (boiling point or 401 °C).

	Operating Point [°C]	TED - Weight (kj/kg)	TED - Volume (MJ/m^3)
$NaNO_3$	380	845	1910
$MgCl_2$ KCl NaCl (37/20.5/42.5)	401	771	1388
$NaNO_3/KNO_3$ (60/40)	401	592	1065
KNO_3	400	536	1132
Aluminum	401	472	1275

Table 4.7: Candidate thermal energy storage materials ranked by highest total energy density (TED) by weight when heated from 115 °C to the melting point.

	Melting Point [°C]	TED - Weight (kj/kg)	TED - Volume (MJ/m^3)
$MgCl_2$ KCl NaCl (37/20.5/42.5)	385	669	1205
$NaNO_3$	307	548	1239
KNO_3	335	355	928
$NaNO_3/KNO_3$ (60/40)	220	267	480

Table 4.8: Candidate thermal energy storage materials ranked by highest total energy density (TED) by weight when heated from 115 °C to the maximum operating temperature (boiling point or 401 °C).

	Operating Point [°C]	TED - Weight (kj/kg)	TED - Volume (MJ/m^3)
$MgCl_2$ KCl NaCl (37/20.5/42.5)	401	685	1232
$NaNO_3$	380	681	1540
$NaNO_3/KNO_3$ (60/40)	401	484	871
KNO_3	400	440	928
Aluminum	401	359	970

4.3.3 Experimental Setup

The recovery tests completed in chapter 3 with the KNO_3 vessels were repeated with the aluminum vessel and sealed vessels containing 5 kg of the four candidate energy storage materials - KNO_3, $NaNO_3$, a 60/40 mol% mixture of KNO_3 and $NaNO_3$, and the 60/20.4/19.6 wt% mixture of $MgCl_2$ KCl NaCl. An electric resistance heater, instead of the solar concentrator, was used to charge the vessel to its MOP minus ~20 °C. This offset was added to protect the vessels from overheating. Four temperature data points were recorded for each test: two measured the coldest point of the vessel, one measured the water being heated, and one alternated between ambient and the next liter to be heated. Water boil tests were carried out immediately after heating for each vessel. In brief, successive 1 L pots of distilled water were brought from room temperature (20 - 25 °C) to 95 °C. The tests were concluded when the temperature of the water failed to reach 95 °C. The resultant temperature and time data were then used to calculate the energy recovered and power output of the vessel. In addition, several storage tests were completed with the 60/40 mol% mixture of KNO_3 and $NaNO_3$ and the resulting data was analyzed in a similar manner.

4.4 Results

4.4.1 Instantaneous - Without Storage

Table 4.9 reports the energy recovered from each material. The energy recovered on a volume basis, was calculated using the density of the thermal storage portion of the vessel. The density calculated from components 3, 4, and 5 from figure 4.2 was ~2000 kg/m^3. The energy recovered from the aluminum test was used to calculate the recovered energy from the aluminum portions of the four candidate materials. The energy contained in 2.08 kg of aluminum, adjusted for the different MOP ranges, was subtracted from the energy recovered from each material. An estimate of the energy stored in the vessel was reported. This estimate was calculated by considering the amount of energy stored in the heat transfer system and the energy storage material from the operating temperature to 25 C.

An example temperature profile during the water boil test and the associated water temperature

Table 4.9: Summary of the average energy recovered from the candidate materials. Italics text indicates a calculated result. The test measured the energy recovered from the vessel, which included the heat transfer system and the energy storage material.

	Vessel					Storage Material	
	Operating Temperature C	*Energy Stored* MJ	Recovered Energy MJ	*Recovered Energy* kJ/kg	*Recovered Energy* MJ/m^3	*Recovered Energy* kJ/kg	*Recovered Energy* MJ/m^3
$NaNO_3$	360	5.0	2.93	396	794	487	1101
$NaNO_3/KNO_3$ (60/40)	380	4.1	2.66	360	722	428	771
KNO_3	380	3.4	2.35	318	638	366	773
Aluminum	385	3.9	2.18	250	675	250	675
$MgCl_2/KCl/NaCl$ (37/20.5/42.5)	380	2.6	1.74	235	472	244	439

is presented for each material in figures 4.4 - 4.3. These figures verify three of the four latent heat materials achieved a full melt. The (37/20.5/42.5) wt% mixture of $MgCl_2$ KCl NaCl was excluded from the remaining results because it did not fully enter the liquid state.

Figure 4.8 reports the average energy recovered for each of the nitrate materials and compares the average energy recovered with and without temperature outliers. While care was taken to have each test at the same initial temperature for a particular material, a few tests had initial temperatures more than one standard deviation outside the mean. Two $NaNO_3$ results and one KNO_3 result were excluded from the averages reported. In both cases, the energy recovered from these vessels were several standard deviations away from the mean when compared to the remaining data points. If we use KNO_3 as a baseline, the difference in the average energy recovered corresponds to one additional liter boiled for the (60/40) mixture of $NaNO_3$/ KNO_3 and two additional liters boiled with $NaNO_3$.

The number of complete boils and the average time to reach each individual boil is displayed in figure 4.9. The time to boil is commonly reported and is an intuitive number for consumers. However, the time to boil does not take into account the initial temperature of the water and therefore does not accurately reflect the energy transferred into the water. Figure 4.10 reports the average power - i.e., energy per unit time - delivered during each test, for each material. Figure 4.11 is figure 4.10 replotted with the error bars removed and connecting lines to help visualize changes in the power output. The cumulative power represents the average power delivered up to the conclusion of that point in the series of water boil tests. Position 5 for instance, is the sum of the energy recovered from boil tests 1 - 5 (the first 5 L of water boiled) divided by the sum of the duration of boil tests 1-5. The cumulative power and trend lines are reported in figure 4.12 and 4.13.

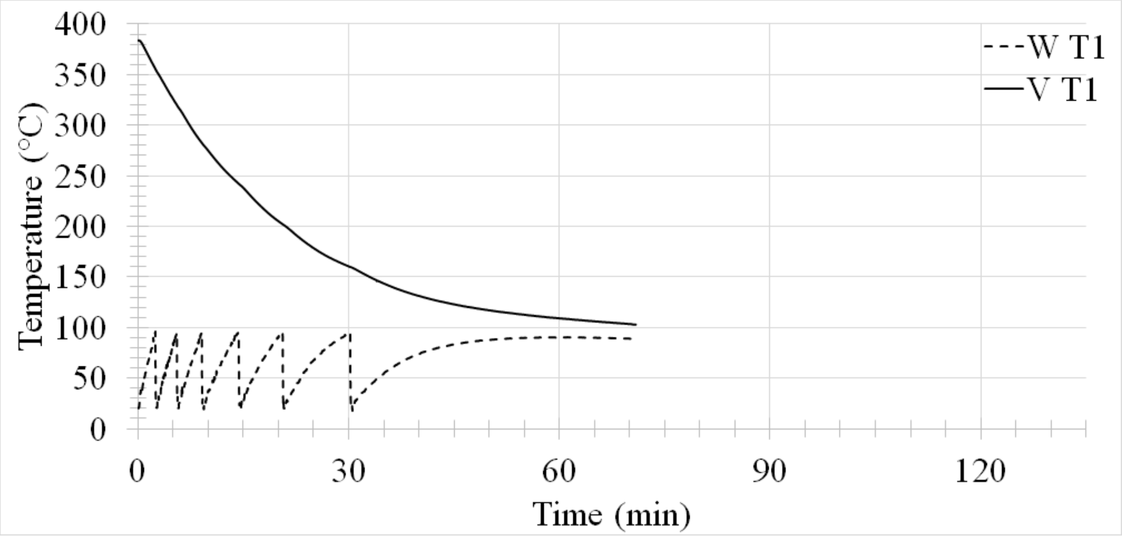

Figure 4.3: Sample output data from the water boil test for the aluminum vessel (V). Six liters of water (W) were boiled with a seventh liter leveling off at 90 °C. This vessel was heated to 384 °C.

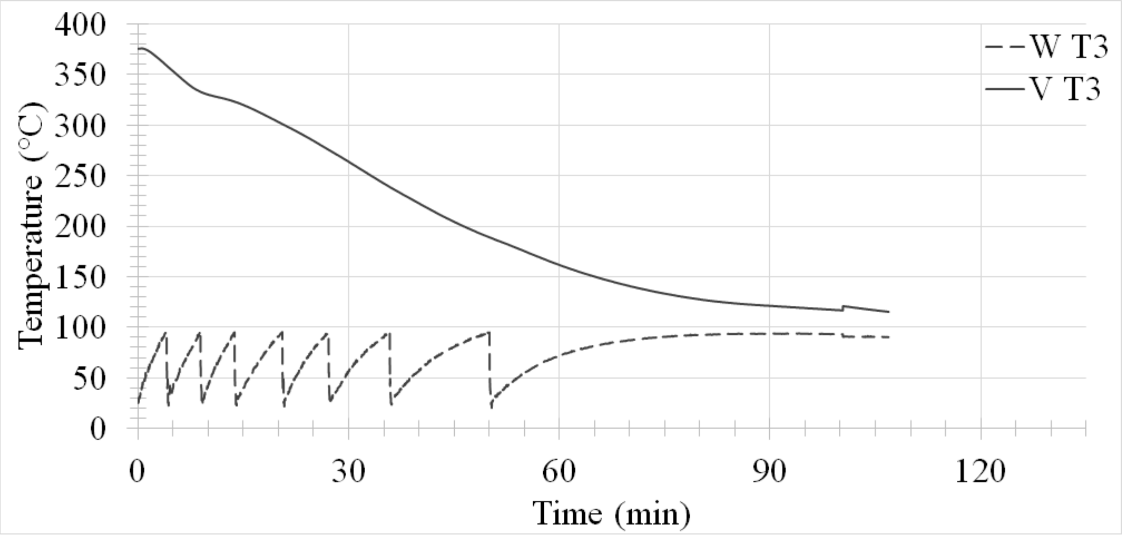

Figure 4.4: Sample output data from the water boil test for the KNO_3 vessel (V). Seven liters of water (W) were boiled with an eighth liter approaching 90 °C.

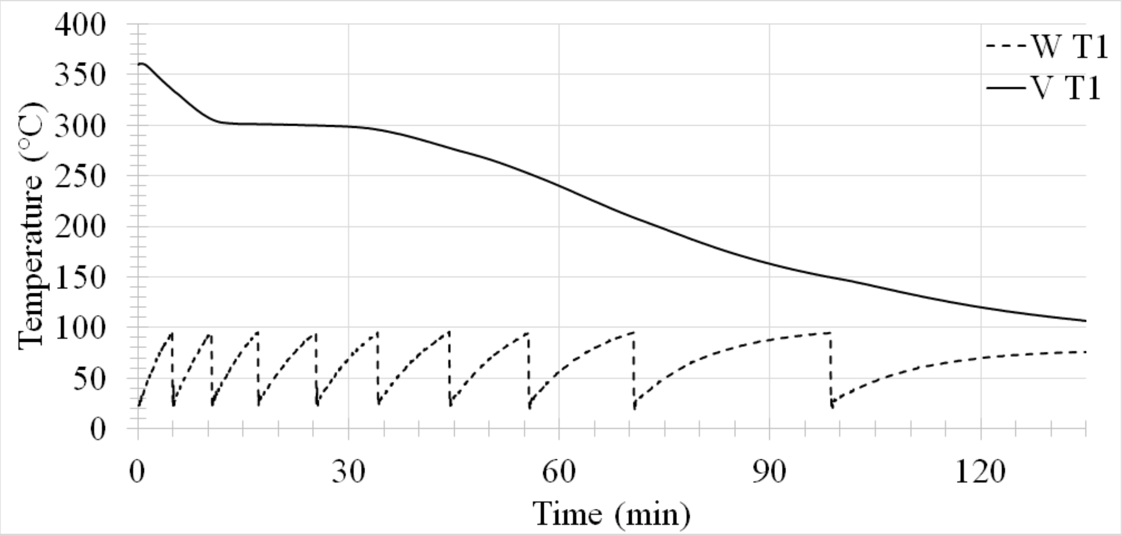

Figure 4.5: Sample output data from the water boil test for the $NaNO_3$ vessel (V). Nine liters of water (W) were boiled with a tenth liter approaching 76 °C.

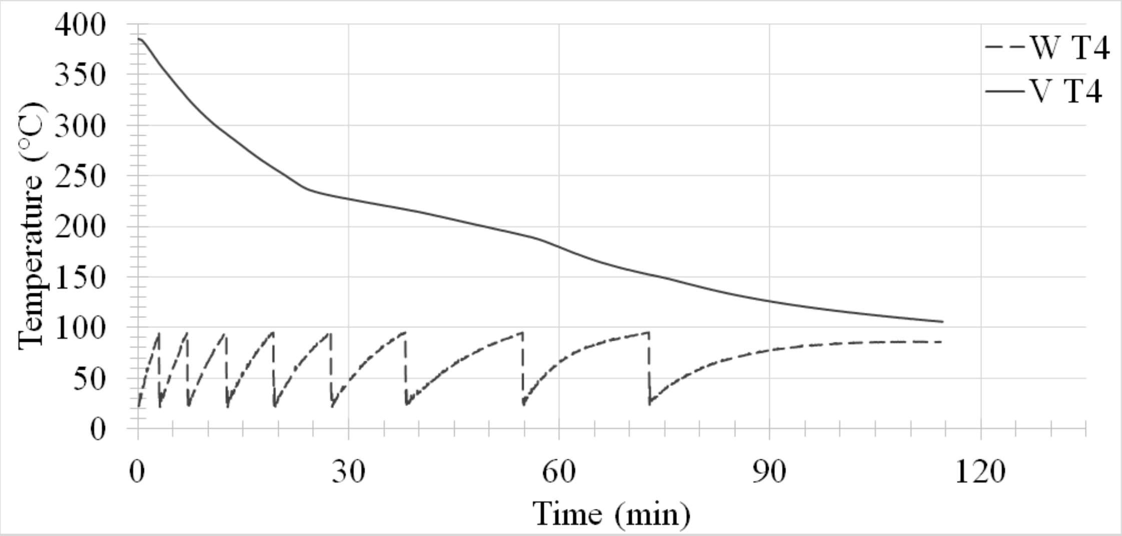

Figure 4.6: Sample output data from the water boil test for the $NaNO_3/KNO_3$ vessel (V). Eight liters of water (W) were boiled with an eighth liter leveling off at 86 °C.

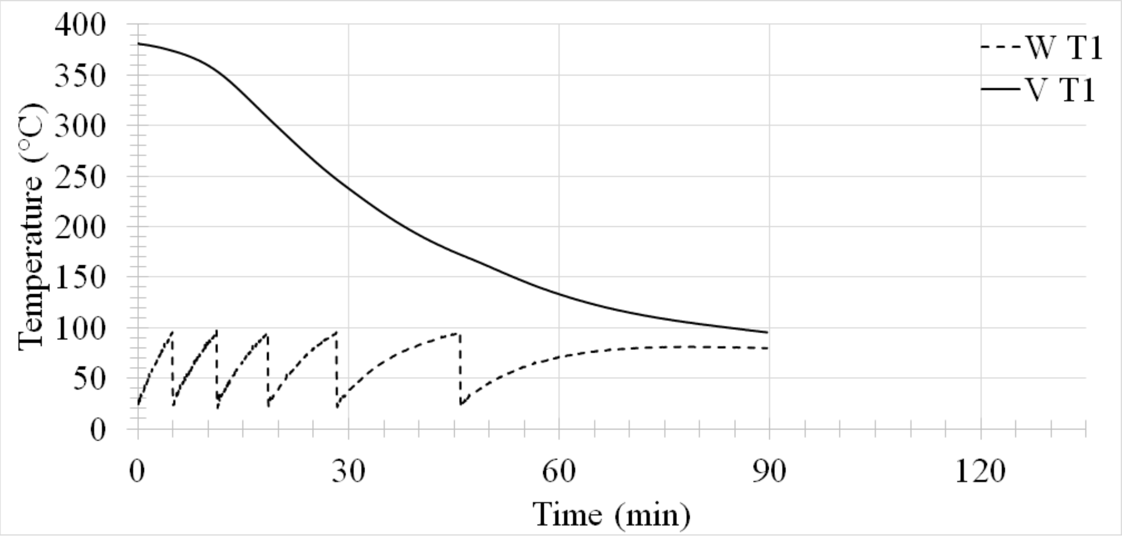

Figure 4.7: Sample output data from the water boil test for the $MgCl_2$ KCl NaCl (37/20.5/42.5) vessel (V). Five liters of water (W) were boiled with a sixth liter leveling off at 80 °C. The material did not make a complete transition into its liquid phase.

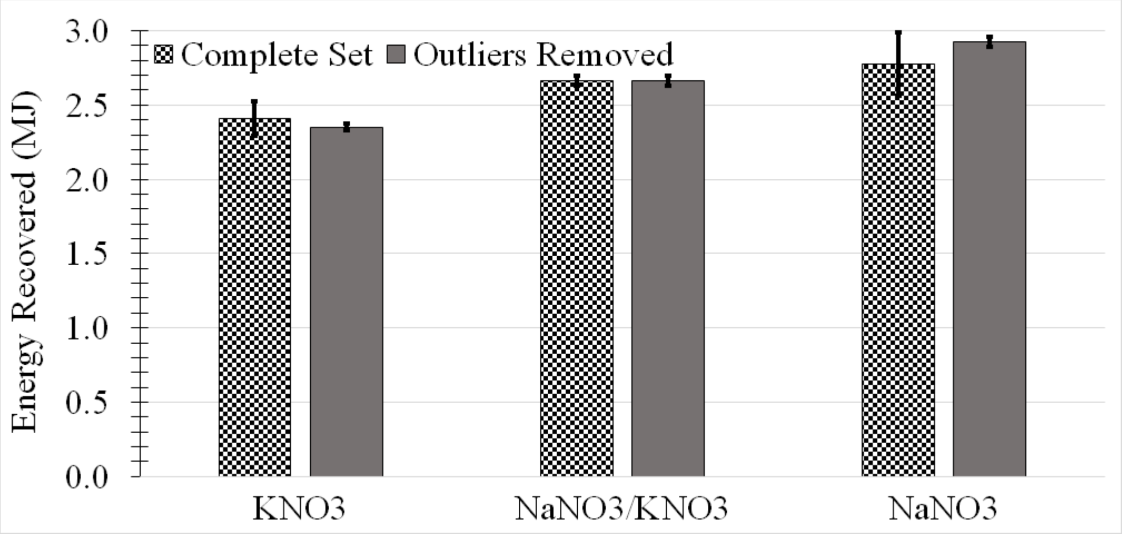

Figure 4.8: The average energy recovered from successive water boil tests for the nitrate materials. $NaNO_3$ had two data points and KNO_3 had one data points removed due to the materials being underheated or overheated respectively. The standard deviation for each range of tests were also reported.

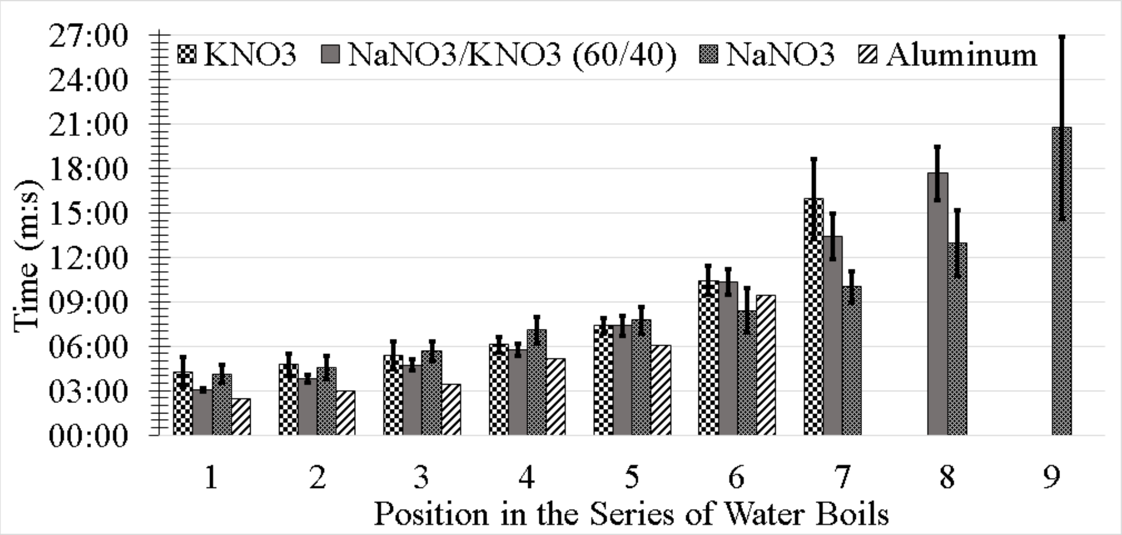

Figure 4.9: The average time to reach each water boil in a series of successive attempts was reported for each material. The standard deviations were also included. The times are reported only for tests when the vessel was heated to within one standard deviation of the mean vessel temperature.

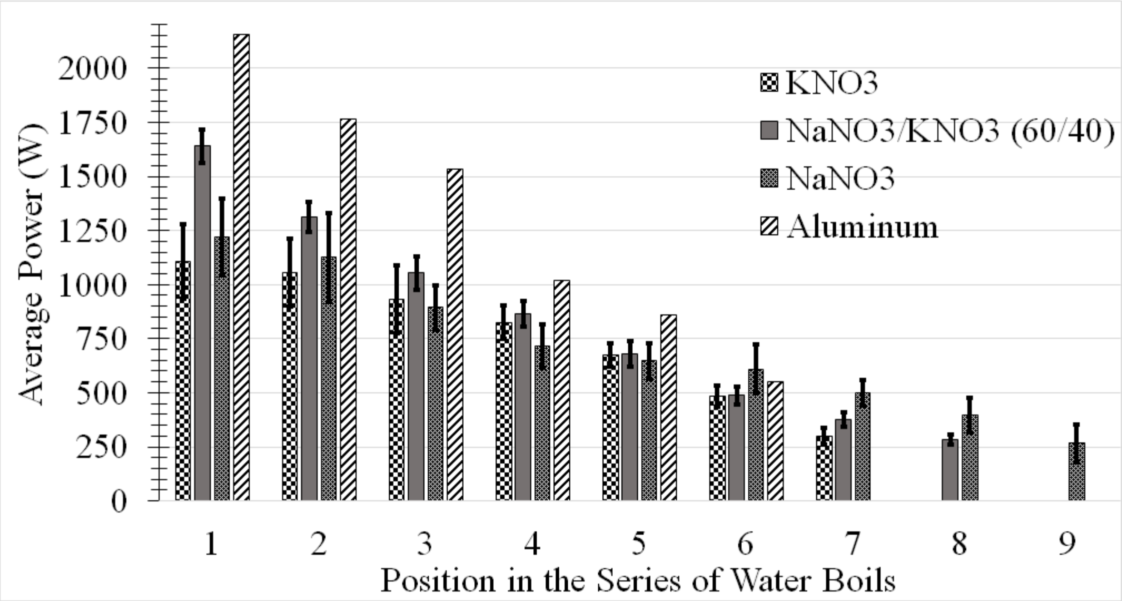

Figure 4.10: The average power output for successive 1 L water boil tests.

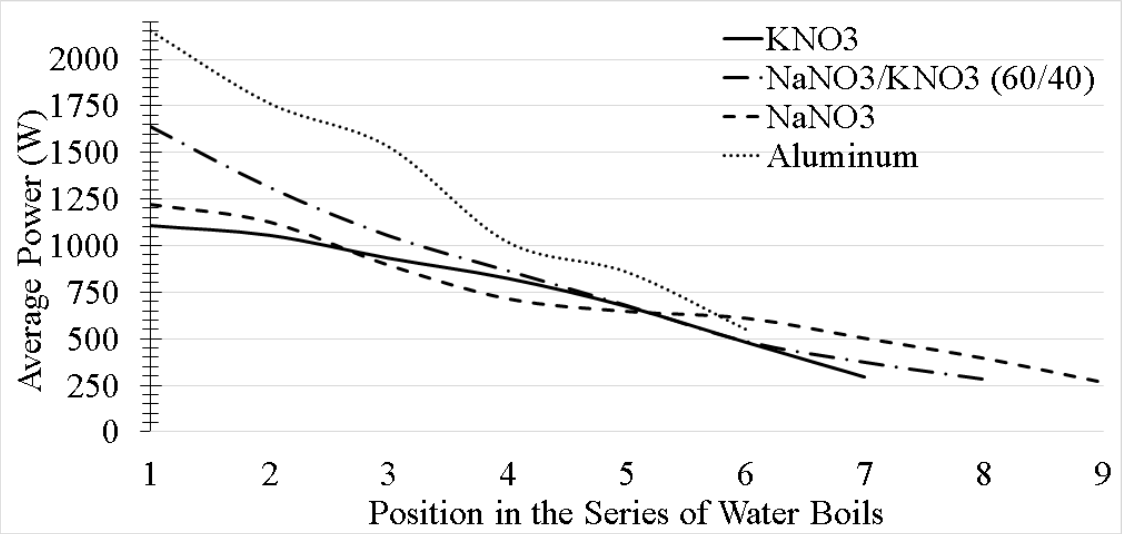

Figure 4.11: The average power output for successive 1 L water boil tests. This is figure 4.10 replotted to visualize the change in power output after each boil.

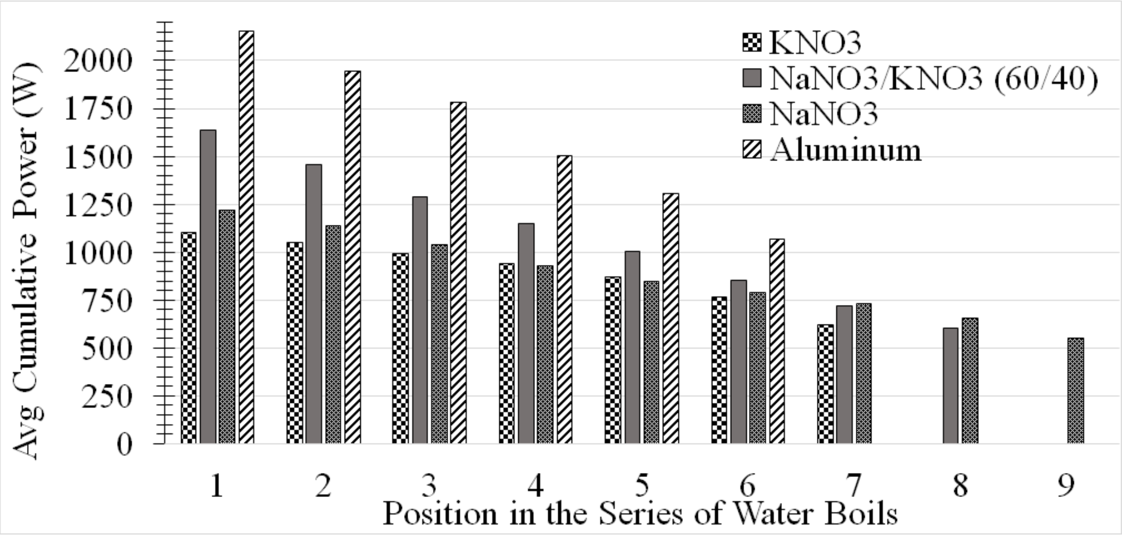

Figure 4.12: Average cumulative power of each candidate material. This represents the average power delivered up to the conclusion of that point in the series of water boil tests.

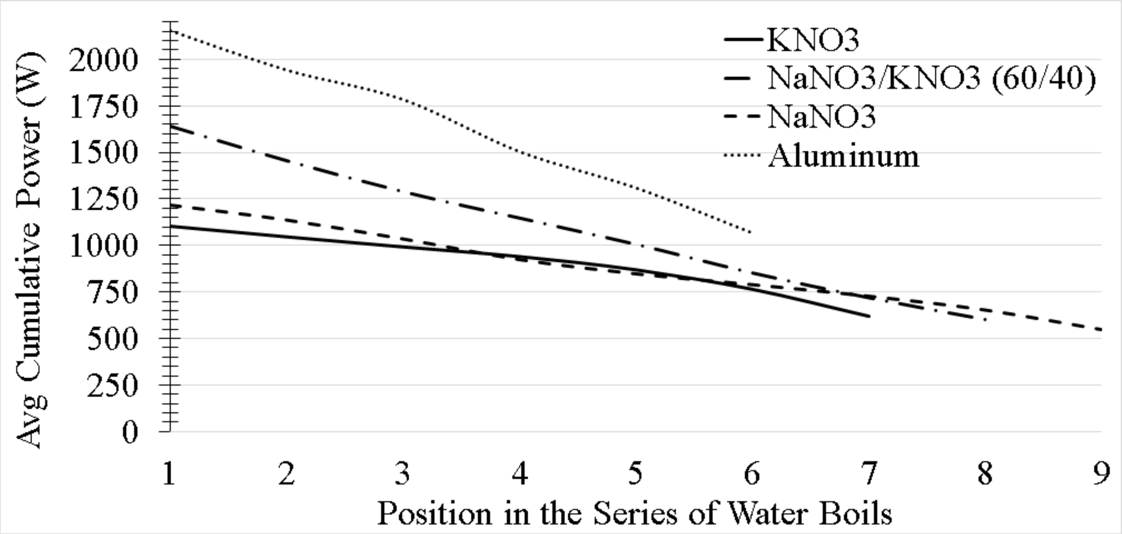

Figure 4.13: Average cumulative power of each candidate material visualized as a line graph to observe trends.

4.4.2 Storage

A series of storage tests were conducted for the $NaNO_3/KNO_3$ (60/40) vessel. The system was heated to the same initial temperature, ~380 °C and stored - allowed to cool - for the specified period of time. The vessel was covered with a lid that was created with 2 inches of Pyrogel insulation. Select water heating and vessel temperature curves are presented in figure 4.14. Between the instantaneous water boil test and the 5 hour storage delay, there was a 1 L reduction in capacity for each hour in storage. The energy recovered from the vessel is reported in figure 4.15. The power results are presented in figure 4.16 and the cumulative power results are presented in figure 4.17. An additional test for each the 5 and 6 hour storage delays were included where the vessel, with the lid, was stored in an insulated container.

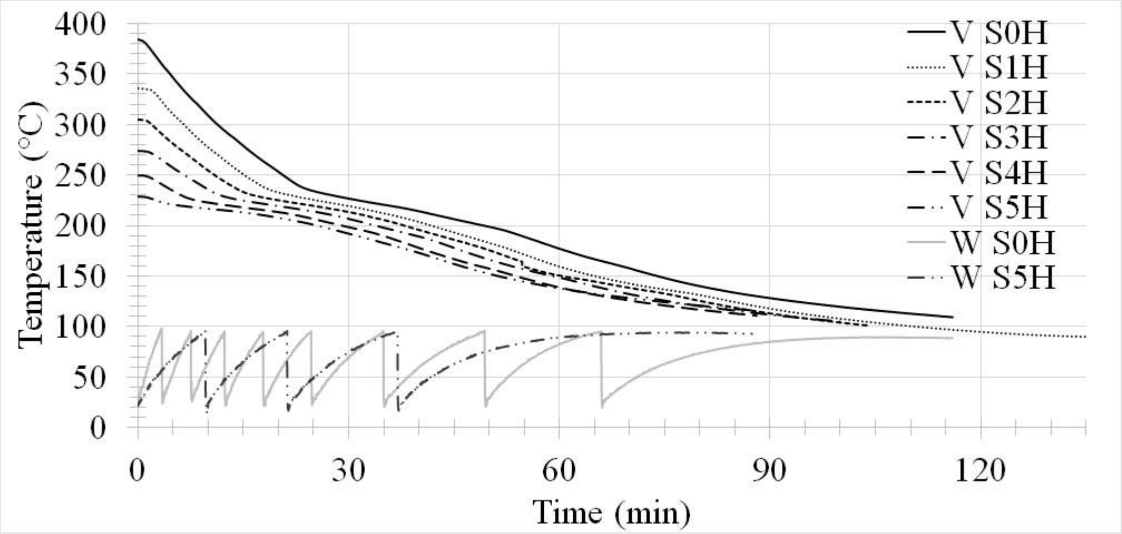

Figure 4.14: Preliminary storage results for the $NaNO_3/KNO_3$ (60/40) mixture. The vessels (V) were stored from 0 hours (S0H) to 5 hours (S5H). The water (W) temperature was reported for the instantaneous (S0H) and 5 hour storage condition.

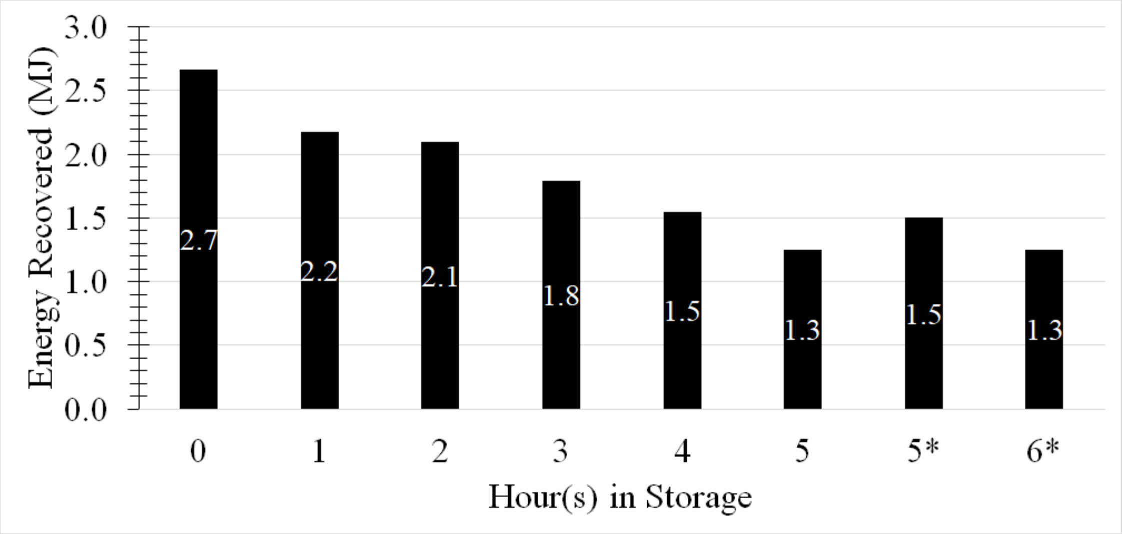

Figure 4.15: Preliminary recovery results for the $NaNO_3/KNO_3$ (60/40) mixture. The vessels were stored from 0 to 6 hours. Vessels with an * were stored in an insulated container.

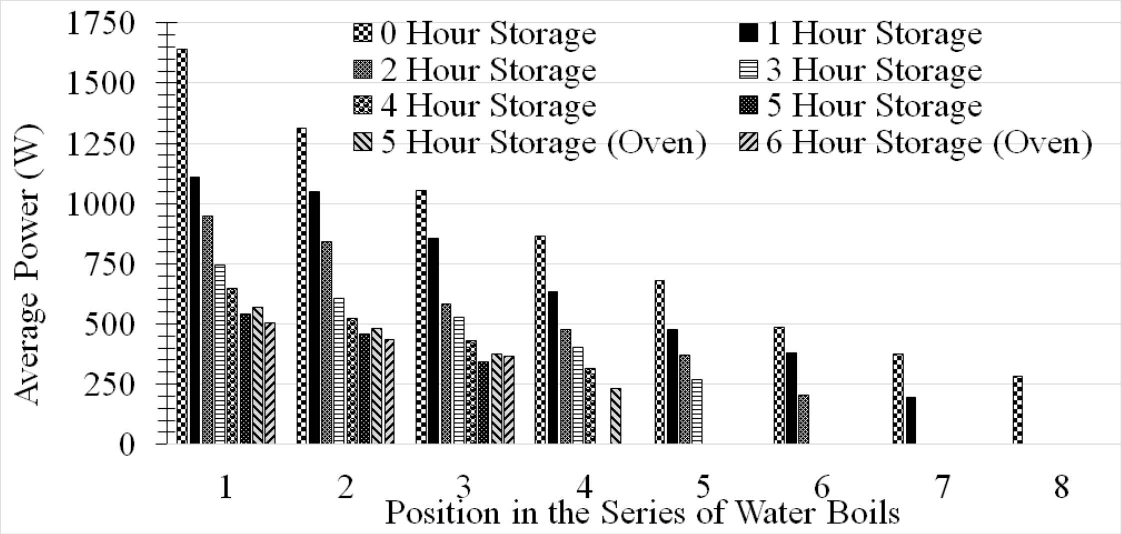

Figure 4.16: Preliminary storage results for the $NaNO_3/KNO_3$ (60/40) mixture.

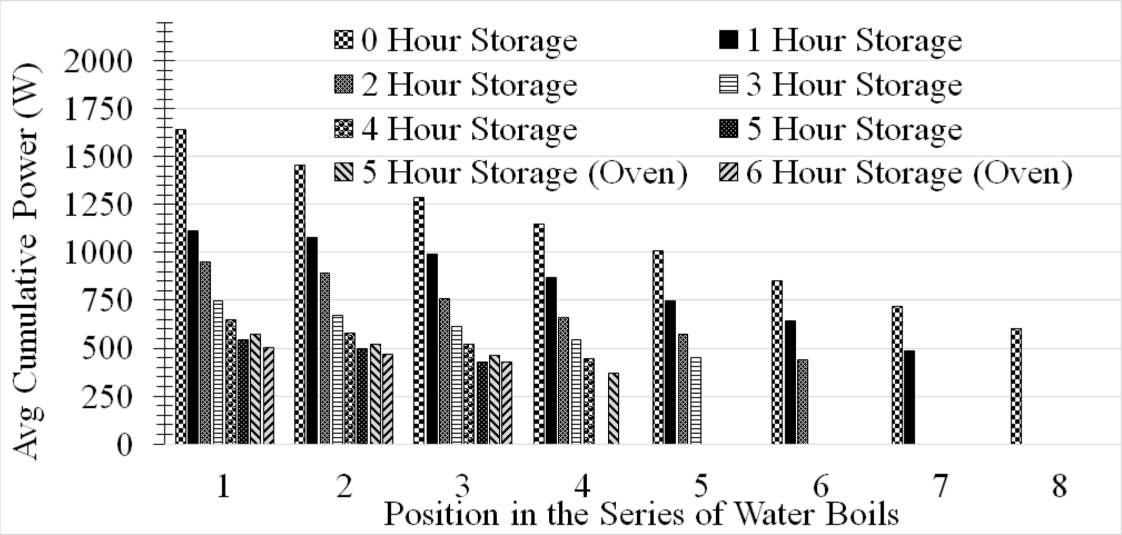

Figure 4.17: Preliminary storage results for the $NaNO_3/KNO_3$ (60/40) mixture.

4.5 Discussion

Five metrics - the temperature profile during energy recovery, time to boil, power, cumulative power, and the total energy recovered - were reported for the KNO_3, $NaNO_3$, a 60/40 mol% mixture of KNO_3 and $NaNO_3$, and aluminum vessels. The temperature profile provides a history of the test and is an essential reference when trying to determine why the material performed as reported. As described previously, the time to boil was reported because it is intuitive for practitioners and laypersons alike to think about the performance. The total energy recovered provides an estimate of the energy or cooking capacity under the prescribed conditions, ~MOP to ~115 °C. The total energy recovered does not provide a complete picture of the performance, this is why it is necessary to report the power.

In this study, power was reported for every liter of water boiled. The power metric tells the user how fast energy is being transferred into the water. The power is dependent on the heat transfer system of the vessel and the heat transfer setup between the vessel and the cookware. Since these tests used the same heat transfer setup, we can compare the expected performance of the materials. A low power result indicates that it is more difficult to transfer heat out of the material and if higher power levels are desired, a more complex heat transfer system would need to be used. The cumulative power can be used to estimate the performance when larger quantities of water are heated. In tests conducted with the nitrate mixture, higher power levels were achieved than what was estimated by this metric but it was a sufficient estimate. The remainder of the discussion focuses on the specific details that may have contributed to the performance of each material. This discussion is summarized in table 4.10.

Table 4.10: Summary of the performance trade-offs between the different materials tested

	Benefit	Deficiency
$NaNO_3$	Energy Capacity	Power Output
$NaNO_3$/KNO_3 (60/40)	Power Output and MOP	Power Stability
KNO_3	Power Stability	Performance
Aluminum	Power Output, MOP, and Solid	Power Stability
MgCl2 KCl NaCl (37/20.5/42.5)	Predicted Capacity	Off-gassing

4.5.1 Instantaneous - No Storage

The solid aluminum vessel was simple to fabricate and performed very well. Recall figure 4.10 compares the power of the nitrate vessels with the aluminum vessel. The aluminum vessel had the highest power output and fastest water boil performance of the materials tested; it only took 20 minutes to boil a total of 5 L of water, in 1 L increments. The 6061 Aluminum has excellent heat transfer characteristics and can transport energy very quickly to the vessel surface and the water.

Energy density and vessel weight is the biggest concern with the aluminum system. It was the heaviest vessel tested and only 2.18 MJ of energy was recovered from the vessel. The high power output would be advantageous for frying, but it would be mismatched where foods are expected to simmer for hours. In communities that use heat retention baskets - where the food would be brought to a boil and then placed in an insulated bag to continue cooking - the simple aluminum cylinder would be very useful.

Recall that the performance of the KNO_3 vessel is reported in figure 4.4. When compared with figure 4.11, it is evident from the slope change that the KNO_3 material completed its phase change by the conclusion of the fourth boil. The average power levels follow a linear trend for the remaining boil attempts. KNO_3 has the lowest heat capacity among the nitrates and the highest melting point, therefore it would be the first mix to undergo and complete its phase change. In addition, it stores the least amount of energy as latent heat. It maintained the highest temperature of the nitrate materials for the first several boils, but not the highest power level. This makes sense since it is supposed to have the lowest liquid and solid thermal conductivity of the nitrates, and its early transition to a solid state limits any convective heat transfer gains from the molten salt. While the KNO_3 vessel was heated to the same temperature as the nitrate mixture and the aluminum cylinder, all three of the candidate materials had a higher initial power output, including the $NaNO_3$ vessel that was heated to a lower temperature. This result further confirms the influence of thermal conductivity and the limited convective influences due to the early phase transition. Though its overall power level was lower than the other materials, it decreases in power at the lowest initial rate as can be observed in figure 4.13. This means it is providing a steadier initial power output until the end of its phase change.

KNO_3 has a lower heat capacity, thermal conductivity, and latent heat of solidification. From a performance perspective, there does not appear to be a strong advantage to use this material over $NaNO_3$. On the other hand, having a higher melting point does make it more difficult to overheat the vessel. In addition, KNO_3 stores a lower amount of energy, therefore it will heat quicker than the other nitrate options. In situations where high levels of energy are not required and the power level is sufficient, it would be a good option to consider when heating the device with solar thermal energy.

Recall that an example vessel and water boil temperature profile for the $NaNO_3$ test is reported in figure 4.5. When compared with figure 4.11, it can be observed that it completed its phase change at the end of boil 6. At the bottom of the vessel it began the phase change in between the second and third boil. We can observe a similar slope between the 1st and 2nd boil and after the 6th boil. Implying that the sensible heat is dominant in these ranges. During the 2nd boil, the temperature is reduced and the material begins transitioning to a solid throughout the vessel. The remaining superheat is exhausted by the end of the third boil and a section of steady power is released between the 4th and 6th boils. $NaNO_3$ has two steady power outputs, ~1200 W until the end of the second boil and ~600 W between the 4th and 6th boils, when used under the test conditions. It also contained the most energy, with approximately 2.9 MJ being recovered. It could be an ideal material for briefly frying foods and could provide a strong simmer for a large quantity of food. The larger capacity of energy storage of course requires a longer time to heat, given the same conditions and equipment.

The reason two $NaNO_3$ tests had to be removed was because the vessel was overheated and the top plate became convex. This was due to a malfunctioning hotplate that may have caused the $NaNO_3$ to boil. Since the sidewalls and bottom surface are constrained by the insulation and a binding wire, the pressure is exerted on the cooking surface. The mechanical properties of aluminum, at this temperature, are significantly reduced and this increase in pressure caused it to deform. The mechanics of heat transfer limit the probability of overheating $NaNO_3$ in practice, but there is a greater chance of overheating when compared to KNO_3 and the (60/40) $NaNO_3/KNO_3$ mixture since they have higher boiling points.

The performance of the nitrate mixture, (60/40) $NaNO_3/KNO_3$, can be reviewed in figures 4.6 and 4.11. It begins with a comparatively high power output and then continues to decline in power with a slight respite as it undergoes its phase change between the 3rd and 6th boil. In this test, the mix had ~150 °C of superheat which allowed for an increased heat transfer rate due to convective forces within the liquid. Additionally, it has the highest thermal conductivity (solid) of the nitrates which may help it continue to release energy quickly even as it begins to solidify along the aluminum heat transfer surface. The mix provided the highest power output when compared to the individual nitrates until its 5th L of water. The nitrate mixture is the most flexible material option. In practice, the charging time and the level of superheat can be balanced by the specific needs of the user in a given day.

The main advantage of the nitrate mix is in fabrication and in risk reduction. In this study the tests were carried out near the MOP of each material to maximize the amount of energy that can be recovered from each vessel. This proved detrimental to the $NaNO_3$ and the chloride mixture as these vessels were damaged due to an issue with overheating. The nitrate mix has a much higher boiling point, ~550°C, so it can be sealed at a much higher temperature than potential users are likely to achieve with a small-scale concentrator. Where small missteps during sealing or reheat could cause the other vessels to be damaged, the nitrate mix provides for a large margin of error in both the use and sealing of the vessel.

The chloride vessel presented a new challenge in vessel sealing because it off-gassed throughout the sealing process. During heating, the material was observed to condense on the ventilation equipment and any high thermal conductivity surface. During the final welding process, the vapor would interfere with and ultimately push out the weld. In order to obtain a seal, the weld needed to be attempted several times as the vessel cooled. It is assumed initial vessels failed without a successful result because they may not have been entirely melted when it was sealed. Another vessel was created by allowing the material to rest for several hours in the molten state. The MOP was exceeded and it was sealed at 425 °C without further difficulty. Unfortunately during heating, the vessel deformed even though it was kept under the sealing temperature. This suggests the material continued to off-gas and pressurized the vessel. A similar chloride vessel in was also overheated and later a cross section was taken, figure 4.18. The small voids indicate only a portion of the salt melted, while the large solid sections verify it never fully melted after the initial sealing. This material appears to be incompatible with the containment methods described in this work. It was expected to have a power characteristic similar to KNO_3 but at a higher power output and with the storage capacity of $NaNO_3$. While several attempts to recover energy from this vessel were recorded, it was clear from the temperature - time graphs that the material did not complete its phase change. As the vessel deformed, it became increasing difficult to heat and improbable that reliable recovery data could be collected.

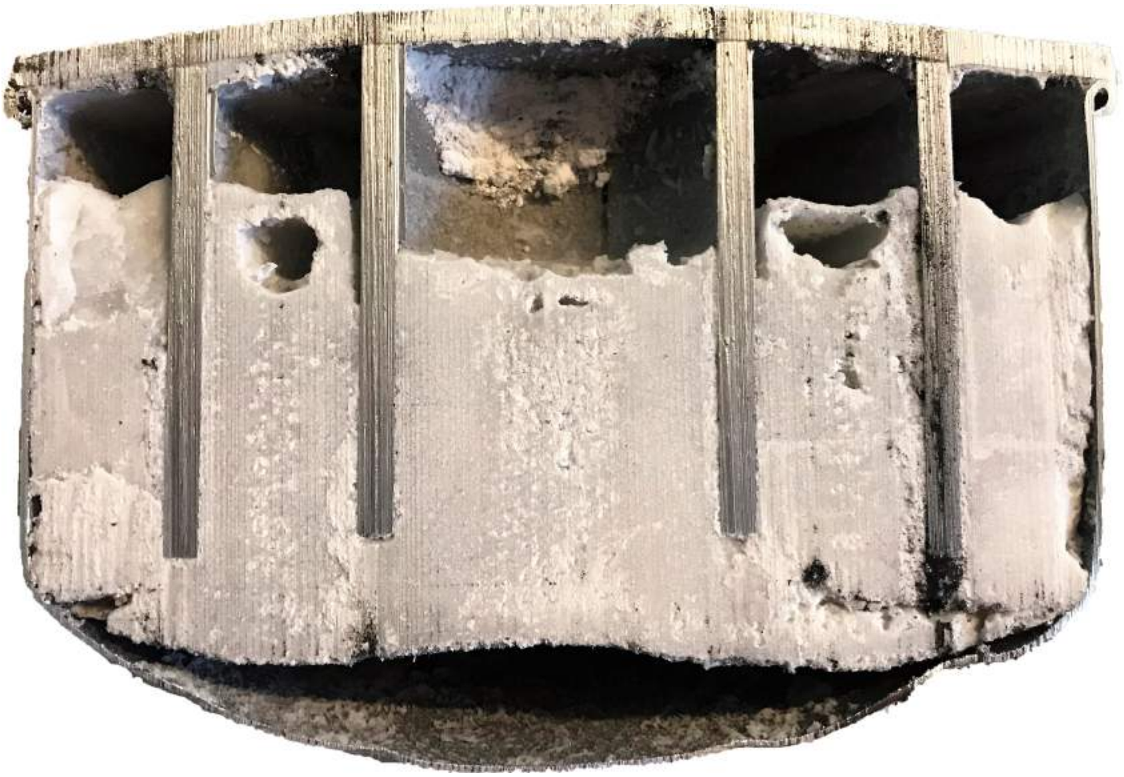

Figure 4.18: Cross-sectional cut of an 8" x 4" vessel filled with $MgCl_2$ KCl NaCl (37/20.5/42.5).

4.5.2 Storage

The storage results for the $NaNO_3/KNO_3$ (60/40) mixture were reported in figures 4.14 - 4.17. In figure 4.14, we can see the 6th liter in the instantaneous test had similar performance as the 1st liter under the 5 hour storage condition. The vessel temperature at the beginning of these two tests were similar. Similarly, the 4th liter of the instantaneous test begins at the same temperature as the 2 hour storage condition. A similar power output is reported in figure 4.16 for these two tests. We can predict the performance in storage by matching the stored temperature of the vessel with the temperature - time graph of a vessel that began a boil at the same temperature.

The result in figure 4.14 also lends evidence that the high power output of the mixture was associated with the liquid phase of the material. The bottom of the vessel for the two and three hour storage conditions had entered the phase change by the end of the third and second boil respectively. The power output is greatly reduced at that point. The vessel under the instantaneous condition entered the phase change near the beginning of the fourth boil, its power level at that point is similar to when the one hour and two hour vessels underwent the phase change.

As observed in figure 4.15, a large portion of the overall energy is lost in the first hour of storage as the energy is transferred into the lid. Between the 2nd and 5th hour of storage, the recovered energy decreases in a linear fashion. In an attempt to increase the energy recovered in storage, two of the test were conducted in an insulated container - a kamado grill - in addition to the Pyrogel insulation and lid. This additional containment increased the number of liters boiled by 1 L.

4.6 Summary and Conclusions

KNO_3, $NaNO_3$, and a (60/40) mixture of $NaNO_3/KNO_3$ were successfully sealed and tested in a portable vessel. Between 2.3 and 2.9 MJ of energy was successfully recovered from these vessels at initial power levels of 1000 to 1650 W. The three systems had similar performance characteristics with each having minor advantages. Specifically, KNO_3 had a fairly stable power output; the largest quantity of energy was recovered from $NaNO_3$; the $NaNO_3/KNO_3$ mixture demonstrated a very high power output that declined in a fairly linear fashion. In addition, while the lowest amount of energy was recovered on a per weight basis from the aluminum vessel, it was competitive in performance and required significantly less effort to produce. Any one of these materials could be used successfully to cook one or more meals for a small family, save a significant amount of cooking fuel, and prevent the release of harmful pollutants.

A high power range of 1600 - 2150 W was achieved by the nitrate mix and the aluminum cylinder. The convective heat transfer and high thermal conductivity respectively, were more important than the temperature of the system in achieving a high power output. While most of the lower temperature materials were excluded for high cost or expected cycling complications, the performance of the nitrate mixture may justify further review of materials with a phase change in the 200 - 300 °C range that have an MOP at or above 400 °C.

KNO_3 and $NaNO_3$ are easily accessible and easy to work with. They do not require special precautions when heating such as inert atmospheres, desiccants, and can work effectively when used alone or when combined. Similarly, aluminum provides a very high performance option with minimal manufacturing effort. These materials can extend the use of solar thermal cooking devices and provide an effective means to cook when the sun is no longer available.

5 Developing Metrics to Evaluate Solar Thermal Storage Systems

5.1 Introduction

The purpose of this section is to discuss key issues related to developing a standard for comparing the performance of stored solar thermal energy cookers. As discussed in sections 1.2.1 and 1.2.2, there is not a standard method to report the performance of these devices. This section will not address the social or cultural issues that need to be considered for the successful adoption of stored solar thermal cookstoves, just the performance aspects.

5.2 Background

When considering the performance of a solar cooking system there are two main questions to consider: how well the system captures the available sunlight and how much of that energy can be used? The amount of sunlight available can be determined with a pyranometer and by observing the amount of time spent collecting the solar energy. There are two general methods to consider for determining how much energy is recovered from a solar cooker: a water boil test that measures the sensible heat recovered or a water boil test that measures the latent energy expended. The amount of available sun and the amount of energy recovered can be used to calculate the overall efficiency of the system. From the data collected when measuring the recovered energy, the power output of the system can be calculated. Since the energy collected will not be used immediately, the concept of storage needs to be incorporated into these tests. The storage time is the amount of time after a vessel is removed from solar collection until the energy is recovered.

The ASAE S580.1 standard measures the sensible heat recovered. ASAE S580.1 reports a standardized cooking power by measuring the temperature difference for a fixed quantity of water, 7 L, over a set period of time, 10 minutes [41]. In order to compare solar cookers in areas with varying solar irradiation, the ASAE standard reports the results by normalizing them to a standard solar radiation value of 700 W. The latent method determines the cooking power by measuring the amount of water that is evaporated after a fixed amount of time at the boiling point [42]. It was developed as a simple method to measure the cooking power of concentrating cookers as this method only requires a scale to weigh the water. These test results are also normalized to a standard solar irradiation value. The two methods cannot currently be used to compare stored thermal energy systems as they do not consider storage time nor can the charging and recovery aspects be separated using these methods. In addition, these standards focused on a set amount of water that should be heated. This doesn't allow for users to determine how a product will fit their particular cooking situation, unless it matches the situation chosen for the standard.

The ASAE standard is the most commonly cited performance standard and it continues to be applied to solar cooking systems. It forms the basis of the Solar Cookers International Performance Evaluation Process released in 2017 [43]. Specific issues with s580.1 in regards to stored solar thermal systems are as follows:

1. Section 6.1: The cooking load is based on the intercept area. When considering a stored system, the intercept area and collection time determine the amount of energy available for collection but not the useful energy of the system. The cooking load and intercept area should not be linked for a stored energy system.

2. Section 7.2: The cooking power is specified over a 10-minute interval. This interval works for the large load specified by the standard, but as indicated in section 1.2.4 the consumer satisfaction was not a consideration. As determined in figure 4.10, the power output of a thermal energy storage material can vary considerably over a series of small quantities of water. Further, when looking at the cumulative power level, as observed in figure 4.12, after 7 L the KNO_3 and the nitrate mix have the same average power level even though they would have provided that energy in a different manner. In a general cooking scenario, the nitrate mix would likely have performed better but the user wouldn't be able to tell based on the results from the 7 L test specified in the standard.

3. Section 7.4: The cooking power is normalized for a specific solar insolation value. Similar to the previous issues, the cooking power does not directly link to the solar insolation when

considering storage.

5.3 Methods

The performance of a system can be evaluated more generally by determining how efficiently the system can convert solar energy into useful work. Rather than try to standardize the solar insolation and make every system conform to a standard quantity of energy, we can measure the amount of energy available to the system and how much energy is recovered from the system at a certain time period and in a scalable manner. In addition, this allows the purchaser to compare solar thermal cookers to photovoltaic systems and other forms of energy use. Cost and performance will be the driving factors in the mind of the consumer, but efficiency is necessary to compare the performance of systems and verify design improvements.

To understand and compare systems, key variables are necessary. The collection method of section 3 and the performance metrics in section 4 have been used to determine these parameters. A set of preliminary design variables and test specific variables are listed below:

1. System variable
   (a) Intercept area [m^2] (based on the entire footprint of the device and not solely what is used for collecting solar radiation)
   (b) Area of the Cooking Surface [m^2]
2. Test specific variables
   (a) The solar irradiance during charging at regular time points [W/m^2]
   (b) Total energy recovered from the system at various storage times [MJ]
   (c) The period of time over which the energy is recovered [s]
   (d) Initial water temperature [°C]
   (e) Ambient air temperature [°C]

The above list captures the basic information necessary to compare the performance of a stored thermal energy system.

The intercept area accounts for the total amount of solar radiation displaced by the device, not just the amount that is concentrated by the device. The system described in chapter 3 blocks a portion of the available energy incident on the dish with the heat storage vessel, and by using the intercept area we can account for that inefficiency. Additionally, a reflective charging system might reflect over 80% of the solar energy incident on it, while a plastic Fresnel lens of the same area might only allow 70% of the energy to reach the device. Similar conditions on available solar insolation as s580.1 may need to be implemented, but they need to be reconsidered for weather. A balance will need to be met between the repeatability of results and the influence the restrictions may have on system design. If the tests only occur in fair weather, then there is an incentive to design systems that only work well under ideal conditions. Alternatively, the restrictions may just need to be clearly stated. The intercept area is multiplied by the average solar irradiance during charging to calculate the amount of available solar energy.

The amount of total energy recovered can be measured immediately or after a storage delay. The amount of total energy recovered can be measured with a water boil test. The test described in section 3, a succession of 1 L water boil tests showed how the performance changes as energy is extracted from the system. In chapter 4 it was observed that the average power level over 7 L can be similar, but the power level and therefore the cooking experience over that time period can be drastically different. While the goal is to calculate the amount of energy recovered, using several discrete amounts of water provides a higher level of detail and is more flexible than the 7 L standard in s580.1. Further testing may indicate less than 1 L of water is more useful and could be used to further compare systems with similar 1 L results. With a portable system, the energy recovery test can be conducted indoors or outdoors. The test should occur in the same manner as the target population would use the cooker.

The power output reported in chapters 3 and 4 did not consider the size of the cooking surface as the system was sized similar to a mid-sized burner on an electric or gas range. To compare dissimilarly sized cooking surfaces, it may be better to report the heat flux [W/m^2] of the system. This is accomplished by dividing the power output by the area of the cooking surface. Unfortunately, the result would be unfamiliar to the general public and would only be useful as a comparison between systems.

The system efficiency, as calculated in chapter 3, is used because it encompasses all possible losses a system might experience. It is calculated by taking the energy recovered after a specified delay and dividing it by the total available solar energy during heating. Further development is necessary to determine an appropriate delay, but 1 hour intervals can serve as an initial starting point. In section 4.4.2, storage tests were conducted with the nitrate mixture and the first few hours of storage correlated to 1 L per hour loss in total boiling capacity. Local context can be used to drive the decision in regards to the storage delay. The delay period can be adjusted to align with meal times and omit sleep periods. Reporting the system efficiency over several delay periods will provide the community with useful information when determining what energy technologies to use.

Cooking is complex and the nature of different cooking styles (pan fry, bake, boil, deep frying, etc.) can be inconsistent across cultures. The amount of energy and the temperature needed to deep fry bread in the US Native American community will be different than the requirement to fry bread in another culture. Each culture may have their own definition of what the taste and texture of the finished product should be like. The power output is necessary to understand the cooking performance of a particular cooker and can be used to compare it to a particular activity within a cooking culture. The results in chapter 4 provided this information as a graph and calculated the power for a series of water boils, repeated for each time delay as it was demonstrated in figure 4.16. The need to measure power incrementally is justified by the similar performance of KNO_3 and the $KNO_3/NaNO_3$ mixture over 7 L. The mixture had a much higher power level initially and would be expected to perform differently than KNO_3 for certain cooking tasks. Reporting the average power level over an arbitrary number of boils would be a disservice to the solar community. It would be appropriate, however, to choose a certain quantity for a local context that consistently demands a specific cooking task. To compare systems in general, it is better to have a more discrete measurement. The cumulative power level can be used to estimate system performance for specific community needs, an example measurement was reported in figure 4.17.

The three main parameters described above: total recoverable energy, system efficiency, and power are demonstrated graphically in figure 5.1. They vary with the length of storage. The initial system efficiency can be used to judge the charging and recovery characteristics of the system, while the delayed system efficiency will convey information about its heat retention capabilities. To determine its appropriateness for specific cooking tasks, the power output can be used. Exact power guidance is likely to be a local decision based on local cooking hardware and preferences.

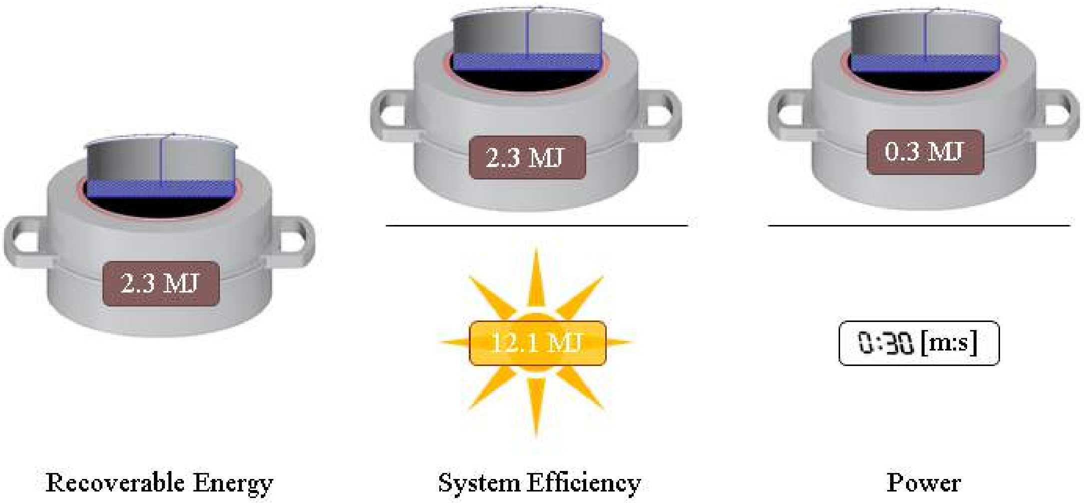

Figure 5.1: A simplified representation of three variables that can be used to describe the performance of a system. The recoverable energy, on the left, forms the basis for measuring the system efficiency and power of the system.

5.4 Conclusions

The variability in cooking styles necessitates a granular and more complex set of variables for comparison than current solar cooker standards report. A quick comparison can be made using the maximum recoverable energy and system efficiency, but a cooking task assessment and comparison to the power outputs will be necessary to determine if a system is appropriate for a family or community. The metrics presented are useful for comparing systems and determining if the system matches the local cooking performance. They do not take into account system costs, social issues, or the cultural context in which the solar cooker is to be situated. Further work is needed to simplify, identify existing, or develop new parameters.

6 Summary and Recommendations

This work briefly reviewed the substantial need for an alternative to solid cooking fuels due to their drastic economic, health, and climate impacts. Interviews with potential users directed this work towards solutions that imitate fire. Interviewees wanted to cook quickly, on demand and in a similar manner as they always have, at a low cost. To achieve a high power output and perform the full range of cooking tasks, it was estimated that the system needed to operate in the 300 - 400 °C range. This range was verified as a useful option but it was determined that it should be expanded to 200 - 400 °C. In the past, there have been significant challenges in matching the cooking culture with solar interventions. This work described an approach to extend the usability of solar energy through a portable thermal storage vessel.

A portable solar thermal energy vessel was designed, fabricated, and tested. The system was heated, in the field, with solar thermal energy and ~19% of the energy incident on an unmodified parabolic concentrator was successfully recovered. The system was further developed and four materials were successfully tested that span the desired operating range: aluminum, KNO_3, $NaNO_3$, and a (60/40) $NaNO_3/KNO_3$ blend. The energy recovered, time to boil, and power outputs were measured. Up to 3 MJ of energy was recovered from a single vessel, a liter of water was boiled in under 3 minutes, and power outputs up to 2150 W (63 kW/m^2) were reported.

Creating a solar thermal cooking system to solve the global cooking problem is a complex undertaking. Otte's variables for adoption can be daunting as user needs have to be satisfied in terms of environmental, cultural, technical, social, economic, and political factors. The vessel and methods described in this work can be used as a platform to test additional energy storage materials. The material set created in this work can then be expanded and these materials can be categorized by their associated cooking characteristics. Potential adopters of this technology would then have an index they could reference and select the appropriate energy storage material for their community.

Further work is needed to increase the duration of storage. Insulation strategies and increased energy densities may be capable of extending the cooking capabilities into lunch the following day, but additional innovations are needed to store energy for a week or through a rainy season. Large scale thermal storage tanks or chemical storage solutions are potential options to investigate.

The technical design and performance of a solar thermal system is only a portion of the work needed to achieve widespread adoption of solar thermal energy. What are the defining characteristics of the user, the food, the cooking process, and the environment that indicate a match? In addition, a charging study will need to be carried out using the candidate materials to determine the advantages and disadvantages of each material in the field.

A significant amount of effort will be required to build the material index for high temperature thermal storage. In addition to this, hundreds of devices already exist in the marketplace. Future work could consider options to incorporate heat storage into these devices that improve the range of cooking options and their acceptability.

The solar cooking community is engaged in finding solutions to the global cooking problem. The portable, stored solar solution demonstrated here is a significant contribution to the community. As this group moves toward a metrics driven discussion, this technical area will continue to grow, reducing our global dependence on the combustion of carbon-based fuels.

7 References

[1] “WHO | Household air pollution and health,” Mar. 2014, 00227. [Online]. Available: http://www.who.int/mediacentre/factsheets/fs292/en/

[2] V. Mishra, “Indoor air pollution from biomass combustion and acute respiratory illness in preschool age children in Zimbabwe,” *International Journal of Epidemiology*, vol. 32, no. 5, pp. 847–853, Oct. 2003. [Online]. Available: http://www.ije.oupjournals.org/cgi/doi/10.1093/ije/dyg240

[3] K. R. Smith, N. Bruce, K. Balakrishnan, H. Adair-Rohani, J. Balmes, Z. Chafe, M. Dherani, H. D. Hosgood, S. Mehta, D. Pope, and E. Rehfuess, “Millions Dead: How Do We Know and What Does It Mean? Methods Used in the Comparative Risk Assessment of Household Air Pollution,” *Annual Review of Public Health*, vol. 35, no. 1, pp. 185–206, 2014. [Online]. Available: http://dx.doi.org/10.1146/annurev-publhealth-032013-182356

[4] D. Mahalanabis, S. Gupta, D. Paul, A. Gupta, M. Lahiri, and M. Khaled, “Risk factors for pneumonia in infants and young children and the role of solid fuel for cooking: a case-control study,” *Epidemiology and Infection*, vol. 129, no. 01, Aug. 2002. [Online]. Available: http://www.journals.cambridge.org/abstract_S0950268802006817

[5] T. C. Bond, S. J. Doherty, D. W. Fahey, P. M. Forster, T. Berntsen, B. J. DeAngelo, M. G. Flanner, S. Ghan, B. Kärcher, D. Koch, S. Kinne, Y. Kondo, P. K. Quinn, M. C. Sarofim, M. G. Schultz, M. Schulz, C. Venkataraman, H. Zhang, S. Zhang, N. Bellouin, S. K. Guttikunda, P. K. Hopke, M. Z. Jacobson, J. W. Kaiser, Z. Klimont, U. Lohmann, J. P. Schwarz, D. Shindell, T. Storelvmo, S. G. Warren, and C. S. Zender, “Bounding the role of black carbon in the climate system: A scientific assessment,” *Journal of Geophysical Research: Atmospheres*, vol. 118, no. 11, pp. 5380–5552, June 2013, 00223. [Online]. Available: http://onlinelibrary.wiley.com.proxy2.library.illinois.edu/doi/10.1002/jgrd.50171/abstract

[6] D. Zaelke and N. Borgford-Parnell, “Primer on Short-Lived Climate Pollutants: Slowing the rate of global warming over the near term by cutting short-lived climate pollutants to complement carbon dioxide reductions for the long term,” Institute for Governance & Sustainable Development, Tech. Rep., 2012. [Online]. Available: http://www.indiaenvironmentportal.org.in/files/file/PrimeronShort-LivedClimatePollutants.pdf

[7] M. Subramanian, “Global health: Deadly dinners,” *Nature News*, vol. 509, no. 7502, p. 548, May 2014. [Online]. Available: http://www.nature.com/news/global-health-deadly-dinners-1.15286

[8] V. R. Putti, M. Tsan, S. Mehta, and S. Kammila, “The State of the Global Clean and Improved Cooking Sector,” Energy Sector Management Assistance Program and the Global Alliance for Clean Cookstoves, Technical Report 96499, May 2015. [Online]. Available: https://openknowledge.worldbank.org/bitstream/handle/10986/21878/96499.pdf?sequence=1&isAllowed=y

[9] J. Masud, D. Sharan, and B. N. Lohani, “Energy for All: Addressing the Energy, Environment, and Poverty Nexus in Asia,” *Open Access Repository*, Apr. 2007. [Online]. Available: https://think-asia.org/handle/11540/225

[10] B. Halacy and D. S. Halacy, *Cooking with the Sun.* Morning Sun Press, 1992, google-Books-ID: WyUoJshS4P8C.

[11] B. Ahmad, “Users and disusers of box solar cookers in urban India: Implications for solar cooking projects,” *Solar Energy*, vol. 69, Supplement 6, pp. 209–215, July 2001. [Online]. Available: http://www.sciencedirect.com/science/article/pii/S0038092X01000378

[12] SCI, “Solar cooker designs,” Oct. 2016. [Online]. Available: http://solarcooking.wikia.com/wiki/Category:Solar_cooker_designs

[13] P. P. Otte, “Solar cookers in developing countries - What is their key to success?” *Energy Policy*, vol. 63, pp. 375–381, Dec. 2013. [Online]. Available: http://www.sciencedirect.com/science/article/pii/S0301421513008793

[14] Rob Goodier, “Challenge: Make a solar cooker that works at night,” Mar. 2011. [Online]. Available: https://www.engineeringforchange.org/challenge-make-a-solar-cookstove-that-works-at-night/

[15] E. Cuce and P. M. Cuce, “A comprehensive review on solar cookers,” *Applied Energy*, vol. 102, pp. 1399–1421, Feb. 2013. [Online]. Available: http://www.sciencedirect.com/science/article/pii/S0306261912006423

[16] M. R. I. Ramadan, S. Aboul-Enein, and A. A. El-Sebaii, “A model of an improved low cost-indoor-solar-cooker in Tanta,” *Solar & Wind Technology*, vol. 5, no. 4, pp. 387–393, 1988. [Online]. Available: http://www.sciencedirect.com/science/article/pii/0741983X88900057

[17] I. Haraksingh, I. A. Mc Doom, and O. S. C. Headley, “A natural convection flat-plate collector solar cooker with short term storage,” *Renewable Energy*, vol. 9, no. 1–4, pp. 729–732, Sep. 1996, 00009. [Online]. Available: http://www.sciencedirect.com/science/article/pii/096014819688387X

[18] R. R. J. v. d. Heetkamp, “The development of small solar concentrating systems with heat storage for rural food preparation,” *Physica Scripta*, vol. 2002, no. T97, p. 99, Jan. 2002. [Online]. Available: http://iopscience.iop.org/1402-4896/2002/T97/019

[19] K. Schwarzer and M. E. Vieira da Silva, “Solar cooking system with or without heat storage for families and institutions,” *Solar Energy*, vol. 75, no. 1, pp. 35–41, July 2003. [Online]. Available: http://www.sciencedirect.com/science/article/pii/S0038092X0300197X

[20] K. Schwarzer and M. E. V. da Silva, "Characterisation and design methods of solar cookers," *Solar Energy*, vol. 82, no. 2, pp. 157–163, Feb. 2008. [Online]. Available: http://www.sciencedirect.com/science/article/pii/S0038092X07001314

[21] Jörg Baur, "Social Acceptance of Solar Stoves in South Africa," Deutsche Gesellschaft für Technische Zusammenarbeit (GTZ) and Department of Minerals and Energy (DME, Tech. Rep., May 2004. [Online]. Available: https://energypedia.info/images/2/28/Solar_Cooking_Compendium_Vol2_Social_Acceptance_GTZ_2004.pdf

[22] Jimmy McGilligan, "Success Story of the Development of a Solar Kitchen at Barli Development Institute for Rural Women using Scheffler Parabolic Dish Community Solar Cookers," July 2006. [Online]. Available: https://vignette.wikia.nocookie.net/solarcooking/images/0/00/Granada06_Mcgilligan_Jimmy.pdf/revision/latest?cb=20070314055641

[23] D. L. Bushnell, "Performance studies of a solar energy storing heat exchanger," *Solar Energy*, vol. 41, no. 6, pp. 503–512, 1988, 00008. [Online]. Available: http://www.sciencedirect.com/science/article/pii/0038092X88900539

[24] D. L. Bushnell and M. Sohi, "A modular phase change heat exchanger for a solar oven," *Solar Energy*, vol. 49, no. 4, pp. 235–244, Oct. 1992. [Online]. Available: http://www.sciencedirect.com/science/article/pii/0038092X9290002R

[25] A. Lecuona, J.-I. Nogueira, R. Ventas, M.-d.-C. Rodríguez-Hidalgo, and M. Legrand, "Solar cooker of the portable parabolic type incorporating heat storage based on PCM," *Applied Energy*, vol. 111, pp. 1136–1146, Nov. 2013. [Online]. Available: http://www.sciencedirect.com/science/article/pii/S0306261913001025

[26] A. Lecuona-Neumann, J.-I. Nogueira-Goriba, and R. Ventas-Garzón, "Solar cooking with heat storage: experiments using PCM and figures of merit for solar cookers," in *International Conference on Advances in Solar Thermal Food Processing*, Faro, Portugal, Jan. 2016. [Online]. Available: http://vignette4.wikia.nocookie.net/solarcooking/images/1/14/Paper-Antonio-Lecuona_Faro_2016..pdf/revision/latest?cb=20160216201550

[27] D. Okello, C. W. Foong, O. J. Nydal, and E. J. K. Banda, "An experimental investigation on the combined use of phase change material and rock particles for high temperature (350c) heat storage," *Energy Conversion and Management*, vol. 79, pp. 1–8, Mar. 2014. [Online]. Available: http://www.sciencedirect.com/science/article/pii/S0196890413007607

[28] M. Mussard, A. Gueno, and O. J. Nydal, "Experimental study of solar cooking using heat storage in comparison with direct heating," *Solar Energy*, vol. 98, Part C, pp. 375–383, Dec. 2013, 00001. [Online]. Available: http://www.sciencedirect.com/science/article/pii/S0038092X13003769

[29] A. H. Tesfay, M. B. Kahsay, and O. J. Nydal, "Solar Powered Heat Storage for Injera Baking in Ethiopia," *Energy Procedia*, vol. 57, pp. 1603–1612, Jan. 2014. [Online]. Available: http://www.sciencedirect.com/science/article/pii/S1876610214015197

[30] C. W. Foong, J. E. Hustad, J. Løvseth, and O. J. Nydal, "Numerical Study of a High Temperature Latent Heat Storage (200-300 0 C) Using Eutectic Nitrate Salt of Sodium Nitrate and Potassium Nitrate," in *Excerpt from the proceedings of the COMSOL users conference, Paris*, Nov. 2010. [Online]. Available: https://www.comsol.jp/paper/download/63804/foong_paper.pdf

[31] C. W. Foong, O. J. Nydal, and J. Løvseth, "Investigation of a small scale double-reflector solar concentrating system with high temperature heat storage," *Applied Thermal Engineering*, vol. 31, no. 10, pp. 1807–1815, July 2011. [Online]. Available: http://www.sciencedirect.com/science/article/pii/S1359431111001074

[32] A. Veremachi, B. C. Cuamba, O. J. Nydal, J. Lovseth, and A. Zia, "Experimental investigation of the thermal performance of a parabolic dish concentrating solar collector," 2015. [Online]. Available: http://repository.up.ac.za/handle/2263/49501

[33] A. Veremachi, B. C. Cuamba, A. Zia, J. Lovseth, and O. J. Nydal, "PCM Heat Storage Charged with a Double-Reflector Solar System," *Journal of Solar Energy*, vol. 2016, pp. 1–8, 2016. [Online]. Available: http://www.hindawi.com/journals/jse/2016/9075349/

[34] M. Mussard and O. J. Nydal, "Charging of a heat storage coupled with a low-cost small-scale solar parabolic trough for cooking purposes," *Solar Energy*, vol. 95, pp. 144–154, Sep. 2013, 00000. [Online]. Available: http://www.sciencedirect.com/science/article/pii/S0038092X1300234X

[35] M. Kenisarin and K. Mahkamov, "Solar energy storage using phase change materials," *Renewable and Sustainable Energy Reviews*, vol. 11, no. 9, pp. 1913–1965, Dec. 2007. [Online]. Available: http://www.sciencedirect.com/science/article/pii/S1364032106000633

[36] M. M. Kenisarin, "High-temperature phase change materials for thermal energy storage," *Renewable and Sustainable Energy Reviews*, vol. 14, no. 3, pp. 955–970, Apr. 2010. [Online]. Available: http://www.sciencedirect.com/science/article/pii/S1364032109002731

[37] S. Kuravi, Y. Goswami, E. K. Stefanakos, M. Ram, C. Jotshi, S. Pendyala, J. Trahan, P. Sridharan, M. Rahman, and B. Krakow, "Thermal energy storage for concentrating solar power plants," *Technology & Innovation*, vol. 14, no. 2, pp. 81–91, 2012.

[38] J. Gomez, G. C. Glatzmaier, A. Starace, C. Turchi, and J. Ortega, "High Temperature Phase Change Materials for Thermal Energy Storage Applications: Preprint," National Renewable Energy Laboratory (NREL), Golden, CO., Tech. Rep. NREL/CP-5500-52390, Aug. 2011. [Online]. Available: http://www.osti.gov/scitech/biblio/1024059

[39] T. Bauer, L. Dörte, K. Ulrike, and T. Rainer, "Sodium nitrate for high temperature latent heat storage," 2009. [Online]. Available: http://elib.dlr.de/59385/

[40] J. C. Gomez, "Change Materials (PCM) Candidates for Thermal Energy Storage (TES) Applications," *Contract*, vol. 303, pp. 275–3000, 2011. [Online]. Available: http://www.nrel.gov/docs/fy11osti/51446.pdf

[41] American Society of Agricultural and Biological Engineers, “ASAE S580.1 NOV2013 Testing and Reporting Solar Cooker Performance,” Nov. 2013. [Online]. Available: http://vignette2.wikia.nocookie.net/solarcooking/images/f/f9/ASAE_Standard_S580.1_%28Nov_2013%29.pdf/revision/latest?cb=20150721205417

[42] Solar Cookers International, “Chandak: Development of Universal Standards for Solar Cookers for Use at Test Centers,” Sacramento, Ca, July 2014. [Online]. Available: https://www.youtube.com/watch?v=7-mEBefLKPQ&index=19&list=PL9jFrMzhGWQUgpVKAeNuTN5DhDs5gPACr

[43] Alan Bigelow, “Development of a Performance Evaluation Process (PEP) for Solar Cookers,” Muni Seva Ashram in Goraj, Vadodara, Gujarat, India, Jan. 2017. [Online]. Available: https://vignette.wikia.nocookie.net/solarcooking/images/7/71/1._Alan_Bigelow.pdf/revision/latest?cb=20170309025239

A Detailed Material Lists

A.1 Solar Melting of KNO_3 and $NaNO_3$

1. Solar Burner from Cantina West - 1.5 m^2 Parabolic Concentrator
2. Sol Source from One Earth Designs - 1 m^2 Parabolic Concentrator
3. RDXL4SD 4 port thermocouple data logger from Omega
4. K-type, glass braid, 20 gauge thermocouples (5SRTC-GG-K-20-72) from Omega
5. Sodium nitrate (002/07-US), refined grade in prill form from SQM North America
6. Potassium nitrate (001/06-US), refined grade in prill form from SQM North America
7. 8"x4" 16 gauge, Anodized Aluminum round cakepan from Fat Daddio's
8. Rust-Oleum Specialty Model 7778830
9. 2050 W hot plate, model HP932A from Wenesco
10. MP-200 Pyranometer Separate sensor with handheld meter from Apogee Instruments-

A.2 KNO_3 Solar Heating and Recovery Testing

1. Parabolic cooker from Eco-Worthy - 1.5 m^2 Parabolic Concentrator
2. NI CompactDAQ 4-Slot USB chassis with two 16-channel thermocouple input modules
3. Omega RDXL4SD 4 port thermocouple data logger
4. Omega K-type, glass braid, 20 gauge thermocouples (5SRTC-GG-K-20-72)

5. Omega OB400 thermocouple cement
6. Potassium nitrate (001/06-US), refined grade in prill form from SQM North America
7. 8"x4" 16 gauge, anodized aluminum round cakepan from Fat Daddio's
8. Rust-Oleum Bar-B-Que Black Satin High Heat Spray Paint, Model 7778830
9. SOLKOTE HI/SORB-II from the Solar Energy Corporation (www.solec.org)
10. MP-200 Pyranometer separate sensor with handheld meter from Apogee Instruments
11. 3/8" male pipe - hex socket plug, item 9-5409-06 (www.pressureconnections.com)
12. 6061 Aluminum 10"x6'x.25" sheet from mcmaster.com
13. 6" and 3" OD x .25" Wall x 3.75" 6061-T6 extruded aluminum tube (www.onlinemetals.com)
14. Pyrogel XT-E High temperature insulation